



Politecnico di Torino

Corso di Laurea Magistrale in Ingegneria Aerospaziale

A.a. 2020/2021

Tesi di Laurea Magistrale

Sessione di Laurea Ottobre 2021

Emissions analysis routine for subsonic aircrafts using biofuel

Relatori:

Nicole Viola

Roberta Fusaro

Davide Ferretto

Candidato:

Riccardo Biasco



**Politecnico
di Torino**

Index

List of figures	1
List of tables	2
List of symbols	3
Introduction	4
Chapter 1	5
1 Aviation environmental impact and alternative fuels	
1.1 Emissions from air transport	7
1.2 Actions for emission control and potential reduction	10
1.2.1 ICAO LTO cycle legislation	12
1.3 Biofuel, types, characteristics and production technologies	13
1.3.1 Biofuel production processes	15
1.3.2 Biofuel sources of supply	18
Chapter 2	22
2 Emissions calculation on mission profile: ICAO database and Fuel Flow method II	
2.1 ICAO data bank and LTO cycle prescriptions	23
2.2 ICAO database correction	25
2.2.1 Fuel flow correction	25
2.2.2 CO & Nox emission index correction	29
2.3 CO2 emissions calculation method	31
2.4 Fuel Flow Method 2	33
2.4.1 EI correction with altitude	36
2.4.2 Fuel Flow correction with altitude	39
2.4.3 Data interpolation and mission analysis	42
2.4.3.1 JET-A1	44
2.4.3.2 CSPK (100%)	45
2.4.3.3 JSPK (100%)	46
2.4.3.4 Results and discussion	47

3 Icao database integration

3.1	Genetic gas generator performance analysis	48
3.2	Emission calculation with correlation based models	55
3.2.1	Nitrogen Oxides	55
3.2.2	Carbon dioxide and water	56
3.2.3	Carbon monoxide	56
3.2.4	Hydrocarbons	57
3.3	Example of calculation	58

Conclusions	64
--------------------	----

Appendix A

Matlab code for Fuel Flow method application	65
--	----

Bibliography	80
---------------------	----

List of Figures

- Figure 1.1** Aviation Market forecast to 2050
- Figure 1.2** Pollutant emissions in relation to fuel and air used for one hour of flight
- Figure 1.3** Schematic Aviation Emissions Reduction Roadmap (IATA)
- Figure 1.4** Life Cycle for kerosene and biofuel
- Figure 1.5** German and Brasil arable land in comparison to land needed for biofuel production
- Figure 2.1** LTO cycle prescribed by ICAO in Annex 16 part II
- Figure 2.2** Thrust, fuel flow and sfc for different blend of CSPK
- Figure 2.3** Thrust, fuel flow and sfc for different blend of JSPK
- Figure 2.4** Emissions characteristic curve CFM56-5°4 using JET-A
- Figure 2.5** EICO LTO cycle for CFM56-5°4
- Figure 2.6** EICO₂ LTO cycle for CFM56-5°4
- Figure 2.7** EIHC LTO cycle for CFM56-5°4
- Figure 2.8** EINO_x LTO cycle for CFM56-5°4
- Figure 2.9** Gas generator scheme
- Figure 2.10** Flow chart of the algorithm used to develop matlab code for emissions calculations
- Figure 3.1** Generic gas generator scheme
- Figure 3.2** Thrust characteristics of typical aircraft engine
- Figure 3.3** Specifications for General Electric CF6-50C2
- Figure 3.4** Trend of the dosage f as a function of the end-of-combustion temperature
- Figure 3.5** Emissions index related to F.F. for CO, CO₂, HC and Nox for JET-A1
- Figure 3.6** Emissions index related to T₂ for CO, CO₂, HC and Nox for JET-A1
- Figure 3.7** Emissions index related to F.F. for CO, CO₂, HC and Nox for CSPK
- Figure 3.8** Emissions index related to T₂ for CO, CO₂, HC and Nox for CSPK

List of tables

Table 1.1	Summary of air traffic indicators
Table 1.2	Main emissions from the combustion process of aircraft engines and corresponding radiative forcing
Table 1.3	Different type of biofuel and carbon emission reduction
Table 1.4	JSPK and CSPK chemical and physical properties
Table 2.1	Biofuel properties
Table 2.2	Thrust, fuel flow and sfc for different blend of CSPK
Table 2.3	Thrust, fuel flow and sfc for different blend of JSPK
Table 2.4	Emission index CO correction [%]
Table 2.5	Emission index Nox correction [%]
Table 2.6	Emission index for CFM International CFM56-5A4 (Airbus A-320), for different type of fuel
Table 2.7	Input parameters for mission profile simulation
Table 3.1	Data and results of simulation for CF6-50C2 using Jet-A1
Table 3.2	Data and results of simulation for CF6-50C2 using CSPK

Introduction

Air transport is an ever-expanding sector, it carries goods and people on a daily basis and represents the most efficient and fastest means of connection in today's world. However, it has limitations; it is necessary, together with technological development, to evaluate different methodologies of approach to the problems arising from the environmental impact. The emissions forecast for the coming years, in parallel with the growth forecast for the sector, make it necessary to search for valid alternatives to reduce and control the amount of substances emitted into the atmosphere. One of these lies in the use of alternative fuels with high efficiency and low environmental impact, for the related life cycle. Among the most popular, due to their peculiarities, there are biofuels.

This research aims to provide a method for assessing the pollutants emitted by air transport and resulting from the use not only of traditional fuels, but also of alternative fuels (drop-in biofuels). Specifically, with the use of pre-existing methods and studies and with the implementation of new calculation algorithms, it is possible to analyze the emissions deriving from a complete flight, modulated phase by phase according to the individual characteristics of a complete mission profile. In order to be able to make the survey iterative, a code in Matlab language has been developed that is capable of carrying out the analysis with the only request of entering some input data.

The first chapter provides an overview of the current and future needs of air transport, growth forecasts and the impact they could have on the environment. The issues relating to the emissions of chemical compounds deriving from the combustion processes of aeronautical engines are discussed and the fuels obtained from biomass are presented in broad terms, focusing on the sources from which they can be obtained, on the production processes and finally on the chemical and physical characteristics of the same. An overview is thus provided which will be characterized in the second chapter by a more accurate description of the peculiarities of the fuels, this time focused on the performance characteristics and the corresponding emission index. A model is also proposed for calculating emissions at high altitude and in general with varying flight conditions. This method is closely linked to the ICAO emissions databank, from which it derives some fundamental parameters. In the case in which it is necessary to disengage from the database, in chapter 3, an alternative model is proposed that exploits empirical relationships to obtain the emission indexes, together with the application of some basic equations of gas dynamics and the application of the performance analysis on design of the aeronautical engine. Finally, in the appendix, the Matlab code generated to complete the simulations and analyzes is proposed and made available.

Chapter 1

Aviation environmental impact and alternative fuels

In 2017, airlines around the world carried around 4.1 billion passengers, 56 million tons of cargo on 37 million commercial flights. Every day, airplanes carry over 10 million passengers and approximately \$ 18 billion in goods. Aviation provides the world's only rapid transit network, generating economic growth, creating jobs and facilitating international trade and tourism. Over the course of the twentieth century, aviation has evolved to become one of the most influential industries on the planet. The sector is constantly growing, and judging by the studies of the International Civil Aviation Organization (ICAO), the trend is practically exponential.

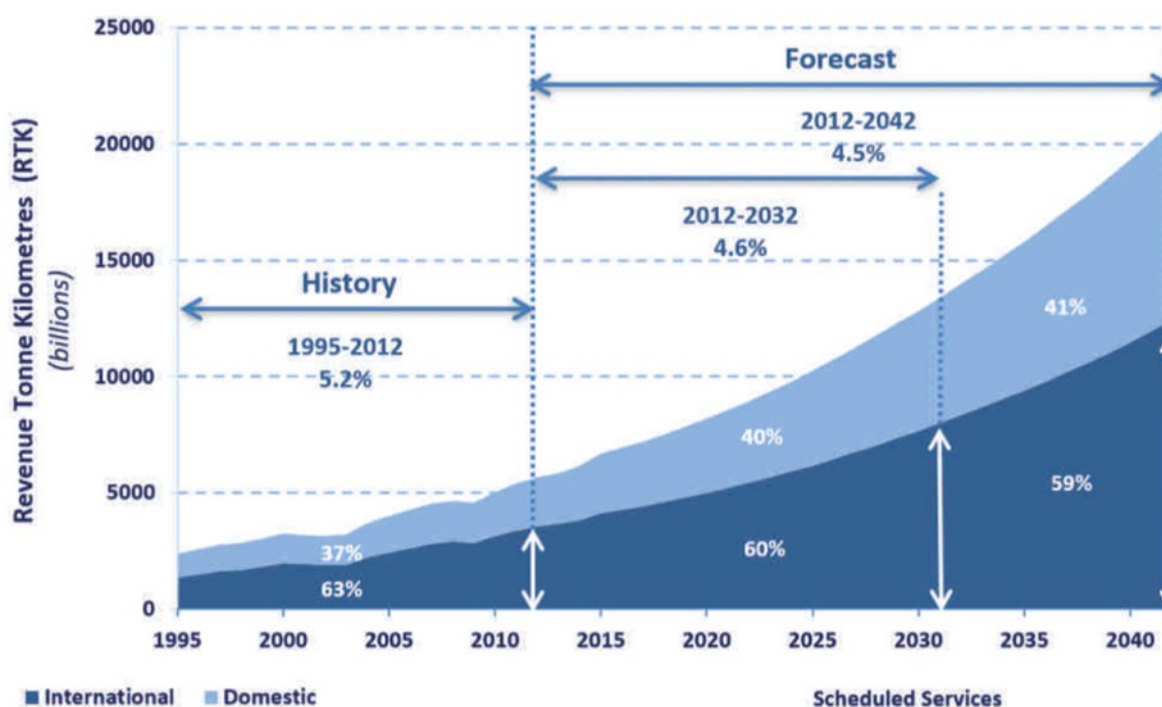


Figure 1.1 Aviation Market forecast to 2050

Together with the increase in flights and fleets, if the situation remained unchanged from a technological point of view, there would be a dizzying increase in airborne pollutants. In 2016, aviation was responsible for 3.6% of total emissions of green house gas (GHG, main responsible for the greenhouse effect) within the European Union and 13.4% of emissions attributable to transport alone.¹

From figure 1.1 and table 1.1 it is possible to see how the aviation market is destined for constant growth. The growing trend is also evident in the data obtained from the European Aviation Safety Agency (EASA), and specifically in the IATA (International Air Transport Association) indicators. Year after year, the number of short, medium and long-haul flights, the number of passengers, the quantities of goods, the distances traveled and the number of airlines, as well as the number of fleets and aircraft per fleet, increase with growth rates of over 50% in some cases. It is therefore necessary and in the common interest to address the issue of sustainability in order to mitigate the environmental impact of the sector.

Table 1.1 Summary of air traffic indicators²

	Units	2005	2014	2017
			(% change since 2005)	
Number of flights ¹	millions	8.89	8.85	9.56
			(-0.4%)	(+8%)
Actual flown distance ¹	billion km	13.1	14.6	16.4
			(+11%)	(+25%)
Average distance per flight ¹	km	1,478	1,649	1,714
			(+12%)	(+16%)
Passengers on commercial flights ²	millions	592	742	890
			(+25%)	(+50%)
Passenger load factor ²	%	70.2	76.7	80.3
			(+9%)	(+14%)
Passengers per flight ²		86	113	124
			(+31%)	(+43%)
Passenger kilometres ^{2, 3}	billion	1,030	1,364	1,643
			(+32%)	(+60%)
Cargo on all-cargo and passenger aircraft ²	million tonnes	6.4	8.3	10.0
			(+29%)	(+55%)
Number of all-cargo flights ¹	thousands	319	305	312
			(-4%)	(-2%)
Average aircraft age ¹	years	9.6	10.3	10.8
			(+7%)	(+13%)

1 Arrivals and departures

2 Departures only

3 Kilometres represent the shortest (or great circle) distance between origin and destination

¹ European aviation environmental report, Colonia, 2019, EASA

² European aviation environmental report, Colonia, 2019, EASA

1.1 Emissions from air transport

Aircraft emit a range of gases and particles which affect the atmosphere. In the context of climate change, the major emissions are CO₂, nitrogen oxides (NO_x), water vapour (H₂O), sulphur oxides (SO_x) and soot. A summary of the atmospheric impacts of these agents and estimates of their associated radiative forcings in 2000 is provided in Table 1.2 Radiative forcing is a measure of the impact of an agent on the energy balance of the earth's atmosphere. It is technically defined as the change in net irradiance at the tropopause (i.e. the boundary between the troposphere and stratosphere) and is measured in watts per square metre (W/m²). A positive number indicates the agent has a warming effect, a negative number indicates a cooling agent.

Table 1.2 Main emissions from the combustion process of aircraft engines and corresponding radiative forcing

Agent	Comment	Radiative forcing (mW/m ²)*	Scientific understanding
CO ₂	CO ₂ is a well-mixed, long-lived (5 – 200 years) greenhouse gas and its warming effects on the climate are relatively well understood.	+25	Good
NO _x O ₃ CH ₄	NO _x emissions have warming and cooling effects. The warming arises because aviation NO _x emissions result in the production of ozone (O ₃) (a greenhouse gas) in the troposphere. The cooling effects arise because chemical reactions associated with NO _x remove methane (CH ₄) (a greenhouse gas) from the atmosphere.	+22 -10	Fair Fair
H ₂ O H ₂ O Contrails Cirrus	Aviation H ₂ O emissions have three main impacts. H ₂ O emitted from aircraft builds up in the lower stratosphere and traps infrared radiation, leading to warming. Aviation H ₂ O emissions create contrails, which act like clouds and trap heat. Contrails created by aircraft can lead to the creation of cirrus clouds, which also leads to warming.	+2 +10 +30 (range +10 to +80)	Fair Fair Poor
SO _x	SO _x emissions lead to the formation of sulphur aerosols, which reflect solar radiation and thereby cool the atmosphere. They can also have indirect effects by altering cloud formation. The radiative forcing estimates only consider the direct effects.	-3.5	Fair
Soot	Soot can act as a warming agent by trapping and radiating heat. It can also have indirect warming effects by altering the albedo (reflectivity) of the earth's surface. The radiative forcing estimates only consider the direct effects.	+2.5	Fair
Total (without cirrus cloud effects)		+48	

According to the data reported by the member states of the United Nations Framework Convention on Climate Change (UNFCCC), the annual carbon dioxide emissions of all flights operating in the areas of the European Union increased by 95% - from 88 to 171 million tons - between 1990 and 2016. Future emissions, according to the same studies, will vary by + 21% in 2040, or reaching 198 million tons. Similarly, the nitrogen monoxide produced in flight annually increased from 313,000 to 700,000 tons from 1990 to 2016, and is expected to reach 1000000 tons in 2040³. The amount of these emissions, which contribute to the greenhouse effect, obviously contribute to the rise in the average earth temperature, with disastrous and well-known consequences on the ecosystem. It is estimated by the Intergovernmental Panel on Climate Change (IPCC) that by the year 2100 the world will see a temperature change of 2.5–7.8 °C above the average for the years between 1850 and 1900⁴.

The effects of emissions into the atmosphere can be grouped into three macro categories⁵:

- **Direct GHG emissions (CO₂ and H₂O).**

Combustion of fossil fuel results in the formation of CO₂ gas which is typically released as engine emissions. For every kilogram of fuel burned, 3.155 kg of CO₂ are formed. It is accepted within the scientific community that these fossil fuel emissions have resulted in increases in atmospheric CO₂ levels⁶.

Carbon dioxide is a gas with high thermodynamic and photochemical stability, and consequently is highly durable over time (100 years) Nowadays, CO₂ emissions from the aviation sector alone constitute 2% of all emissions anthropogenic and 10-13% of emissions deriving from transport in general⁷. Another element of considerable importance is water vapor H₂O, which contributes to global warming. However, the vapor emissions attributable to air transport are negligible compared to those from other sources, such as evaporation from the earth's surface, and also typically the vapor is disposed of in a couple of weeks by precipitation. If these emissions are released at an altitude lower than that of the tropopause, they do not constitute a substantial problem, precisely because the time spent in the atmosphere is, as already mentioned, short;

- **Emissions that can contribute to the formation of GHG (NO_x and CO).**

The nitrogen oxides produced by aviation make up 2% of the total anthropogenic production. The residence time of the molecule varies with altitude: in the vicinity of the tropopause it is 10 times greater than that of the soil. It is usually converted into ammonia HNO₃ after weeks. This causes a considerable influence on the chemical balance of the atmosphere. Reactions that have nitrogen oxides and carbon monoxide as reactants can also generate ozone O₃ as a secondary product. The latter, if present in

³ European aviation environmental report, Colonia, 2019, EASA

⁴ L. Zhang., T. L. Butler, B. Yang, *Recent Trends, Opportunities and Challenges of Sustainable Aviation Fuel*, Green Energy to Sustainability: Strategies for Global Industries, ed. 1, 2020 John Wiley & Sons Ltd., 2020

⁵ M. Shaefer, *Methodologies for aviation emissions calculation – A comparison of alternative approaches towards 4D global inventories*, Berlin University of Technology, German Aerospace Center (DLR), 2006

⁶ D. Daggett, *Enabling Alternate Fuels for Commercial Aircraft*, Cranfield University, 2009

⁷ Intergovernmental Panel on Climate Change: *Aviation and Global Atmosphere*, Cambridge university press, 1999

the stratosphere, acts as a screen for UV radiation, but at lower altitudes it is in effect a green hous gas with a lifetime of the order of weeks;

- **Substances or particulates that influence the formation and properties of clouds**

The combustion inside aircraft engines produces, together with the other elements, soot and sulphate particles. These are negligible compared to the quantities emitted to the ground by other phenomena such as volcanic eruptions; however, their concentration in the atmosphere could influence the generation of ozone, modify the properties of the clouds, their composition and contribute to the formation of cirrus clouds. These are all phenomena that contribute to the greenhouse effect;

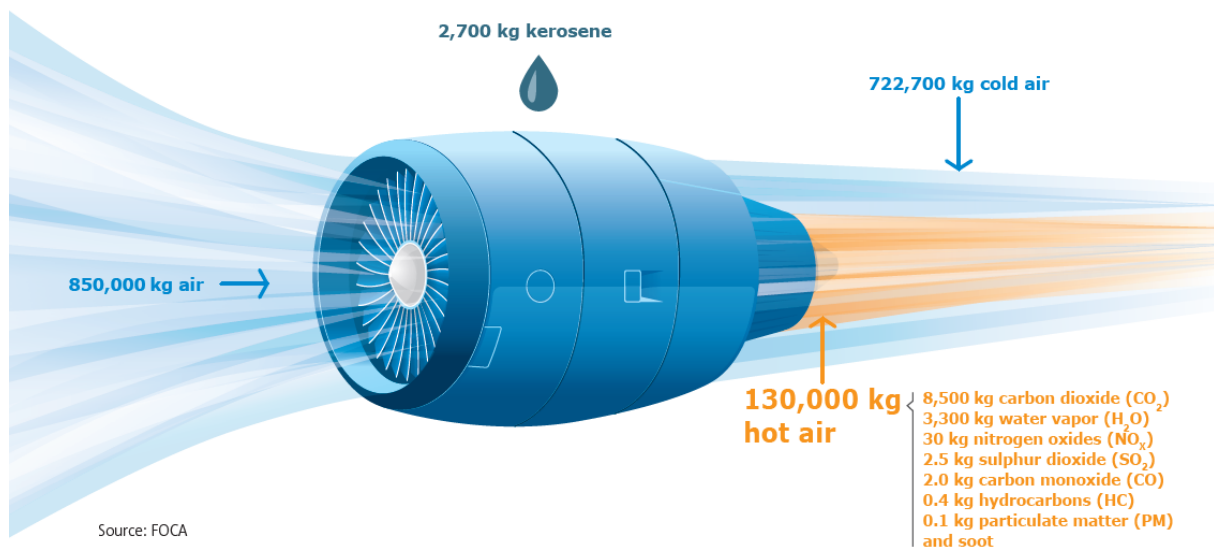


Figure 1.2 Pollutant emissions in relation to fuel and air used for one hour of flight

1.2 Actions for emission control and potential reduction

In 2010, the member states drew up an agreement, through the ICAO, with the intention of increasing the average efficiency of the fuels used by 2% per year, or reducing emissions and imposing a maximum tolerable limit on them. In 2012, an action plan was signed for the first time to outline the policies and guidelines to be universally followed to reduce the impact of aviation on the climate. The initiative of 2012 is followed by that of 2016. In October 2016, the International Civil Aviation Organization (ICAO) stated the new requirements in the Carbon Offsetting and Reduction Scheme for International Aviation (CORSIA) (ICAO's 39th Assembly 2016). CORSIA is an international scheme for regulating CO₂ emissions from Civil Aviation. Its goal is to have a carbon neutral growth from 2020. CORSIA uses Market-based environmental policy instruments to offset CO₂ emissions: aircraft operators have to purchase carbon credits⁸ from the carbon market. Starting in 2021, the scheme is voluntary for all countries until 2027.

At the moment, aviation is not yet one of the main drivers of global warming, but the surge in the growth trajectory of the sector suggests that it could become the decisive factor in the coming decades.⁹

Sustainable mobility is an essential element for social and economic maintenance and development. Air transport must therefore support economic growth by providing a means capable of creating connections while respecting the prerogatives of an eco-sustainable system.

The Advisory Council for Aviation Research and Innovation in Europe (ACARE) has set 5 "goals of flightpath 2050" in order to be able to provide members some guidelines on which to develop future projects, again for the only purpose of ensuring sustainable development:

- The technologies and procedures available in the sector must guarantee a reduction of CO₂ emissions per passenger / km of 75% and a reduction of nitrogen oxide emissions of 90%;
- Taxi maneuvers must guarantee zero emission index;
- Airplanes will be designed and built to be as recyclable as possible;
- Europe will have to establish itself as a center of excellence for the research and use of sustainable alternative fuels, including those for aviation, on the basis of a strong European energy policy;
- Europe must be at the forefront of atmospheric impact research and must take the lead in formulating a priority environmental action plan and in defining global environmental standards;

Obviously, in order to achieve these objectives set for 2050, the configuration and operation of aircraft will need to be gradually and significantly changed.¹⁰

⁸ A carbon credit or carbon credit is a negotiable certificate, or a security equivalent to one ton of CO₂ not emitted or absorbed thanks to an environmental protection project carried out with the aim of reducing or reabsorbing global emissions of CO₂ and other greenhouse gases.

⁹ A. Macintosh, L. Wallace, *International Aviation Emissions to 2025: can emissions be stabilised without restricting demand?*, Canberra, 2008, pp 5-6

¹⁰ Strategic research and innovation agenda, 2017 update, Advisory Council for Aviation Research and Innovation in Europe, Derby, 2017, pp 48-60

It is essential in today's landscape to carry out research and optimize the times in order to provide new methodologies for approaching the problem of environmental sustainability. To make possible the objectives set for the near future, it is necessary to improve and integrate the existing systems and known technologies. Aviation, as suggested by ACARE, can reduce CO₂ emissions by improving the efficiency of fuel, technology, operations and infrastructure, but also by making it possible to use alternative and sustainable fuels (as in the case of biofuels , which will be discussed later). Fuel efficiency is widely discussed, a factor that indicates the average fuel consumption usually referred to a single passenger per kilometer. If this value is not increased, as required, by at least 2% per annum, the scenario generated will see a drastic increase in airborne pollutants, a greater demand for fuel in parallel with the growing trend of air transport and a consequent increase in medium prices.

It is therefore in the interest of the aeronautical industry to evaluate alternative fuels that can at the same time increase fuel efficiency and ensure an energy source that does not come from traditional fossil fuels. So the interest of the aviation industry stems from:

- Generation of additional sources;
- Potential cost reduction;
- Environmental advantages;

1.2.1 ICAO LTO cycle legislation

Aircraft engines must comply with the emission standards defined by ICAO in annex 16 volume 2. These regulations contain a limit imposed on the maximum emissions of pollutants, and specifically CO, HC, Nox and soot during a predetermined landing cycle. and take off (LTO).

As an integral part of the certification process, manufacturers must provide data relating to performance characteristics and emissions. All data is made available and public through the ICAO engine exhaust emissions databank.

Specifically, the emissions for each phase are provided by means of an emission index, i.e. in the form of grams of pollutant emitted per kg of fuel burned (fuel consumption is also supplied in kg / s units).

The ICAO standards were generated mainly to have local air quality control available near airports. Therefore, as anticipated, they only concern taxi operations, take offs, climb and landing, i.e. operations that take place below 3000 ft.

Universal standards are also defined for the characteristic thrust of each phase, as well as for the duration of the same. Emissions at high altitudes are omitted from the certification process, and a method for their estimation, together with the requirements for the individual phases, will be presented in the following chapters.

The fuel flow is used to calculate the total gross emissions D_p of each pollutant during the entire LTO cycle. Thrust specific value D_p/F_∞ in g/kN is the relationship between the big missions and the maximum thrust of the engine, and is used as a parameter for the imposition of the upper limits of certification¹¹:

- Regulatory smoke number:

$$83.6 \cdot (F_\infty)^{-0.274}$$

- Regulatory HC level:

$$\frac{D_p}{F_\infty} = 19.6 \left[\frac{g}{kN} \right]$$

- Regulatory CO level

$$\frac{D_p}{F_\infty} = 118 \left[\frac{g}{kN} \right]$$

- Regulatory Nox level:

different value, dependent on date of production, maximum thrust and overall pressure ratio;

¹¹ Environmental Protection, Annex 16, Vol. II, International Civil Aviation Organization, 3 ed., 2008

1.3 Biofuel, types, characteristics and production technologies

The aviation industry uses specific fuels to power thrusters, and these are usually classified as JET-A1 fuels. All fuels must strictly comply with certain specifications, with ASTM providing the most common standards worldwide, also including the category of renewable and sustainable fuels.

A sustainable alternative fuel can be described as one without negative environmental, economic, and social impacts. In addition to having lower lifecycle green house gas (GHG) emissions, sustainable biofuel should not compete with food or fresh water resources or contribute to deforestation, while providing socioeconomic value to local communities where plant stocks are grown. Oil base energy crops that can meet these sustainability criteria include, but are not limited to jatropha, camelina and algae. Based on the recent results of well-to-wheel¹² Life Cycle Assessments (LCA) carried out by Michigan Technological University, Bio-SPK (Synthetic Paraffinic Kerosene) made from jatropha and camelina oils can achieve a reduction of GHG emissions between 65 and 80 percent relative to petroleum derived jet fuel¹³.

Therefore biofuels can potentially reduce GHG emissions and the consequent impact on climate change compared to traditional fossil fuels if we refer to a complete well to wheel life cycle analysis (fig. 1.4).

Achieving the pollutant reduction targets set as targets by international organizations such as the ICAO requires, in view of the use of biofuels for this purpose, an increase in their production and consumption.

Biofuels may theoretically be produced from any type of biomass, i.e. renewable living organism utilizing carbon as a food source. However, the production of biofuels mostly comes from the processing of grasses, plant seeds, and non-edible tree fruits. As a matter of fact, contrary to fossil sources, biomass sources absorb carbon dioxide as they grow in a proportion equivalent to that produced when the fuel is burnt in the jet engine. As a consequence, when the extraction of fossil fuels releases large amounts of CO₂ in the atmosphere, the growth of biomass feedstocks absorbs large amounts of CO₂. This absorption sometimes more than compensates the remaining lifecycle CO₂ emissions associated with the production of biofuels.¹⁴

¹² Well to wheel: it allows to compare fuels for energy analysis and can be used for environmental analysis. The primary objective of this index is to compare different propulsion technologies and fuels with each other. The comparison takes place by relating the effectiveness of the means of transport, the performance of the technology that makes it possible to obtain the fuel and the energy carrier used both to transport it and to store it.

¹³ J. D. Kinder, T. Rahmes, *Evaluation of bio-derived synthetic paraffinic kerosene (Bio-SPK)*, The Boeing Company, Sustainable Biofuels Research & Technology Program, 2009

¹⁴ A. P. Payan, M. Kirby, C. Y. Justin, D. N. Mavris, *Meeting Emissions Reduction Targets: A Probabilistic Lifecycle Assessment of the Production of Alternative Jet Fuels*, in American Institute of Aeronautics and Astronautics, School of Aerospace Engineering, Georgia Institute of Technology, Atlanta, 2015

Current fuel consumption for the entire international aviation sector according to ICAO estimates of 2016 could reach 852 million tons in 2050; and approximately 426 million tons of biofuels would be needed to achieve the objectives set for GHG reduction. However, current production is very small and limited, managing to cover 1% of aircraft fuel consumption worldwide¹⁵.

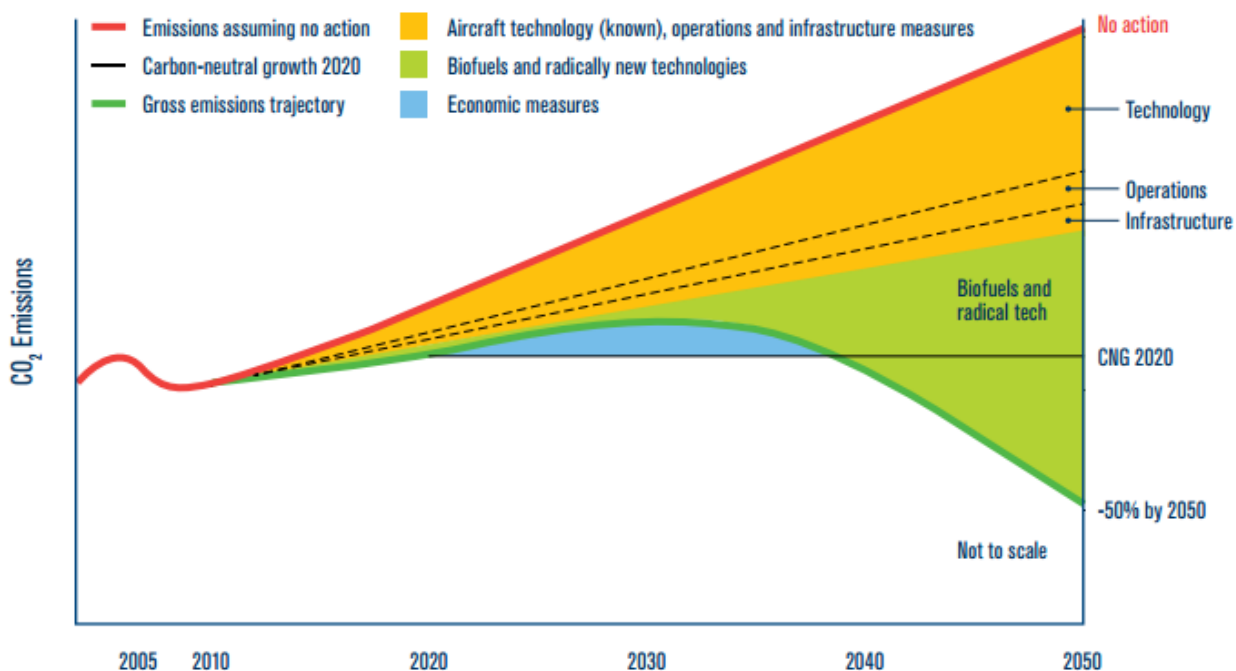


Figure 1.3 Schematic Aviation Emissions Reduction Roadmap (IATA)¹⁶

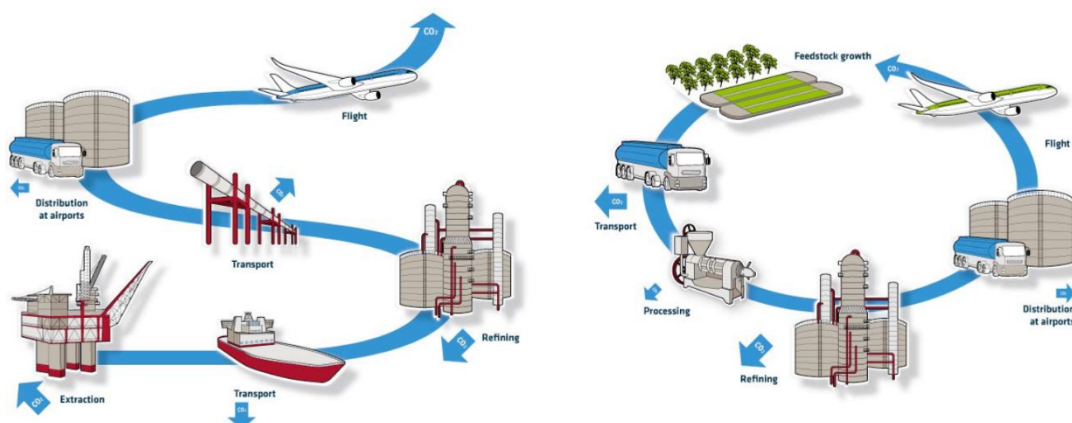


Figure 1.4 Life Cycle for kerosene and biofuel

¹⁵ *Beginners guide to aviation biofuel*, Air Transport Action Group, 2009

¹⁶ *The IATA technology roadmap report*, IATA, 3rd Edition, Montreal, QC, Canada, 2013

The vast majority of biofuels currently available are derived from oleochemical feedstocks (an oleochemical is a chemical compound derived industrially from animal or vegetable oil or fats) such as vegetable oil, animal fat and used cooking oil (UCO).

A further significant advantage in the use of biofuels, regardless of the potential reduction of pollutants and the low environmental impact of their production process, lies in the fact that they can be used on pre-existing aircraft configurations, without the need to make changes. They are called "drop in" fuels. *A "drop-in jet fuel blend" is a substitute for conventional jet fuel, that is completely interchangeable and compatible with conventional jet fuel when blended with conventional jet fuel. A drop-in fuel blend does not require adaptation of the aircraft/engine fuel system or the fuel distribution network, and can be used "as is" on currently flying turbine-powered aircraft.*¹⁷

1.3.1 Biofuel production processes

In May 2016, the American Society for Testing and Materials (ASTM) certified four different processes that can be used for the production of biofuels. As is known, obtaining such a certification affects the possibility of exploiting this technology for powering commercial and international flights.

The certification referred to is the ASTM standard D7566 and officially recognizes 4 production processes:

- Hydroprocessed Esters and Fatty Acids (HEFA bio-jet), are derived from oleochemical feedstocks. They represent the basic concept of biofuels, and were certified in 2011;
- Gasification through the Fischer-Tropsch method (FT), using urban organic waste (MSW) or biomass. It is a high temperature biomass treatment process for the production of a gas which is then used to generate synthetic hydrocarbon fuels over catalysts;
- Synthesised Iso-Paraffinic fuels (SIP). It is a process that involves the fermentation of sugars through microorganisms to create a hydrocarbon molecule called farnesene, which in turn, treated with hydrogen, produces farnesane which is the actual fuel to be blended with JET-A;
- Alcohol-to-jet like the SIP it provides for a fermentation process of sugars in alcohols such as ethanol or butanol and has been certified in 2016;

Nowadays, the majority of bio-fuels currently on the market are HEFA, also because the process used is similar to that used for the production of diesel for road transport and beyond, so several facilities benefit from this production technology.

¹⁷ Sustainable aviation fuels guide, ICAO, 2017

In total, in 2016 the total amount of the global HEFA fuel production capacity was around 4.3 billion liters per year. And if we hypothesize to use this quantity only for the aeronautical market we would be able to cover only 1.5% of the needs of the sector.

One of the reasons why the presence of biofuels is so low in the sector is the cost of production. HEFA fuels have a price that is higher than that of traditional fossil fuels as in the management costs, in addition to production, it is necessary to consider the maintenance prices of the plantations from which the raw materials are obtained. As an example, in 2016 the cost of palm oil (which is the cheapest of all) was 0.45 USD / L, while the price of aviation fuel 0.25 USD / L, practically half. To overcome this problem, several governments (such as Netherlands, Norway, U.S.) are moving towards the implementation of specific policies in order to make it possible to reduce spending on plantation maintenance and conversion processes¹⁸. And it will be precisely these policies that establish the feasibility or otherwise of the objectives set for 2050. In recent years, the number of biofuel-powered commercial flights has increased significantly and a downstream supply chain has been developed in some locations.

Another of the current limits to the large-scale use of these fuels is the lack of mature production technology. The HEFA process has been present for several years and for this reason more developed, but the cost of the raw material, or biomass obtained from plantations, is too high and constitutes 80% of the cost of the fuel itself.

A table (1.3) is shown on the next page, obtained from an EASA report, which highlights the peculiarities of the main biofuels, differentiating them according to the technology adopted for the production process. Specifically, the percentages of possible reductions in carbon dioxide emissions are highlighted.

¹⁸ D. Daggett, O. Hadaller, R. Hendricks, R. Walther, Alternative Fuels and their Potential Impact on Aviation, NASA, October 2006

Table 1.3 Different type of biofuel and carbon emission reduction

Conversion technology	Fuel feedstock	% direct emissions savings compared to fossil-based aviation fuel baseline of 89 gCO ₂ eq/MJ
Fischer-Tropsch (FT)	Agricultural residues	89-94%*
	Forestry residues	88%
	Municipal Solid Waste (MSW)	68%
	Short-rotation woody crops	81%
	Herbaceous energy crops	87%
Hydroprocessed esters and fatty acids (HEFA)	Tallow	78%
	Used cooking oil	85%
	Palm fatty acid distillate	76%
	Soybean	53%
	Rapeseed/Canola	48%
	Camelina	54%
	Palm oil - closed pond	61%
	Palm oil - open pond	29%
Synthesized Iso-paraffins (SIP)	Sugarcane	62%
	Sugarbeet	68%
Alcohol (iso-butanol) to Jet (ATJ)	Agricultural residues	71%
	Forestry residues	74%
	Sugarcane	69%
	Corn grain	54%
	Herbaceous energy crops (switchgrass)	66%
	Molasses	69%
Alcohol (ethanol) to Jet (ATJ)	Sugarcane	69%
	Corn grain	26%

*More than one feedstock considered

1.3.2 Biofuel sources of supply

Biofuels, as mentioned above, are mainly derived from plants, and can be considered sustainable energy sources if a sufficient amount of crops can be grown to meet the demand¹⁹. Unfortunately, several regions or states would not have adequate production capacity, especially in relation to the areas available to be exploited by crops, to meet their own energy needs. For example, the figure below shows that the land available for cultivation in Germany covers 34% of the entire surface of the state.

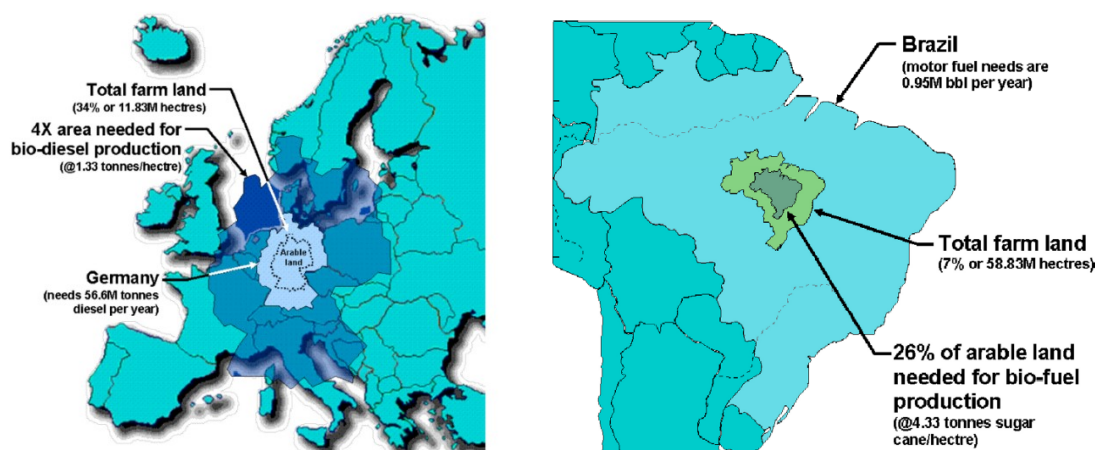


Figure 1.5 German and Brasil arable land in comparison to land needed for biofuel production

To meet the demand for fuel of the same nation, attested to around 56.6 million tons in 2005²⁰, with an equal amount in energy terms of biofuels, a arable area 4 times larger than that currently available would be needed, in addition to the complete replacement of all the crops currently present. However, the situation is quite different in other geographical areas, where the available surface is far greater than that necessary to satisfy the demands of the market, such as Brazil.

Replacing kerosene on a large scale in the aeronautical sector is by no means easy and it is a challenge that various governments have been working on in recent years. As an example, consider that even the global use of blends at 15% by volume of biofuels in JET-A1 is currently impossible. In 2006, the US commercial fleet used approximately 51.5 billion liters of fuel over the course of a year. 15% of annual consumption would correspond to 7.72 billion liters of biofuel. Furthermore, considering that a plantation such as soybean (widely present in the United States) produces about 225 liters of biofuel for each acre (0.0556 l/m^2), 34 million acres of arable land would be needed, or about the entire area of Florida (140 billion m^2)²¹.

¹⁹ *Useful information about conventional and alternate fuels and their feedstocks*, National Renewable Energy Lab, National Bioengineering Center, june 2004

²⁰ Lieberz, S., Germany Oilseeds and Products, Biodiesel in Germany – An Overview, USDA Report #GM2021, October 24, 2002

²¹ D. Daggett, O. Hadaller, R. Hendricks, R. Walther, Alternative Fuels and their Potential Impact on Aviation, NASA, October 2006

Renewable feedstocks are the best raw material from which to start the production of biofuels. The fundamental characteristics of these sources reside in:

- Sustainability;
- Carbon dioxide recycling;
- Renewability;
- Eco-friendly technology;
- Less dependence on petroleum supplying countries;²²

Generically favored sources are derived from crops, plantations, organic waste, forest residuals and halophytes. Among the main ones, the main ones used for the production of biofuel, in relation to their characteristics are:

- CAMELINA

It is a plant widely used for the production of vegetable oil, thanks to its seeds containing a high oil content. The oil content varies between 30 and 40%, and is also a plant that does not need fertilizers for growth, can be grown on poorly fertile soils and is not affected by diseases and insects. The remains resulting from the extraction of the oil can be safely used as animal feed. Furthermore, the production costs, for the reasons listed above, are reduced compared to other crops, and are around 0.10-0.20 \$ / l. In 2012, around 750 million liters of oil were produced in the United States.

-JATROPHA

Like the camelina plantations, the jatropha is a plant species that can grow in marginal land, not very fertile soils, it is a resistant plant and little affected by parasites. It grows rapidly in geographic areas with a favorable climate. However, the waste produced by obtaining the oil cannot be used in the food industry or on farms as it is poisonous, but at the same time it can be exploited for the extraction of nitrogen, sodium and potassium.

- ALGAE

They constitute a valid alternative to remedy the current scarce provision of other sources and vast arable land. They have a high lipid content, a high carbon dioxide absorption rate during their life cycle, low land take and a high growth rate.

The most influential positive side lies in the fact that they do not affect and do not conflict with other pre-existing crops since they do not require the availability of land and especially water for their cultivation.

The remaining biomass as a result of oil extraction can be used for food purposes, as feed for intensive farming, for the production of paper and bioplastics and again for the production of energy.

- WASTES

The waste, as such, comes from different sources, and can be converted into biofuels following different procedures. They are a widely present and economic resource.

²² Bozel JJ. *The use of renewable feedstocks for the production of chemicals and materials-a brief overview of concepts*

Furthermore, usually, above all, municipal organic waste is rich in fats and therefore are suitable for the extraction of oils.

- HALOPHYTES

They are herbs that grow in salty waters, and in environments hostile to other plant species. They are usually readily available in tropical and subtropical areas. Also in this case there is no need to have arable land and moreover, as in the case of algae, obviously they do not require the addition of water, consequently the production costs are very low.

Due to the previous advanced knowledge of production technology and the current level of progress, for this research, it was decided to focus attention on HEFA biofuels, and in particular on those obtained from camelina and jatropha.

The latter choice is linked to the vast availability of information in this regard, such as the chemical properties of the fuel obtained from them with the above methodology. Hydroprocessed renewable jet fuels (HRJs) anche detti hydroprocessed esters and fatty acids (HEFA) are typically paraffinic liquids with molecular formula C_nH_{2n+2} , they are produced by hydrodeoxygenation of vegetable oils and animal fats, and most of the by-products are made up of water and propane. This category of fuels is peculiar for their high combustion energy efficiency and for the possibility of being exploited even in the absence of a second element / mixing fuel. They are free of aromatics and sulfur, have a high thermal stability. They can be used without having to modify the architecture of the engines, they prevent the formation of deposits and corrosion of the constituent elements of the engine, and their combustion is ash free, they retain good properties even at low temperatures, which is why they can also be used at high altitudes. Finally, the molecules are devoid of oxygen.²³

Below is a table that lists the main characteristics and specifications of the fuels taken into consideration. In the following chapters, a detailed analysis of the performance characteristics deriving from the use of the aforementioned biofuels on aircraft engines is dealt with

²³ Hari, Yaakob, Binitha, *Aviation biofuel from renewable resources: routes, opportunities and challenges*, renewable and sustainable energy reviews, 2015

Table 1.4 JSPK and CSPK chemical and physical properties

Properties	Jatropha	Camelina
Density [kg/m³]	864-880	780
Cetane number	46-55	50.4
Viscosity [mm²/s @40°C]	3.7-5.8	3.8
Pour Point [°C]	5	-7
Flash Point [°C]	163-238	136
Lower Heating Value [MJ/kg]	44.4	44
CFPP [°C]	-1.2	-3
Acid Value [mg/KOH]	0.34	-
Cloud Point [°C]	5	3
Oxidation Stability [h]	5	-
Iodine Value [I₂/100g]	109.5	152.8
Sulphur Content [ppm]	12.9	-
Specific Gravity [g/ml]	0.876	0.882
Molecular Formula	C₁₂H₂₆	C₁₂H_{24.5}

Chapter 2

Emissions calculation on mission profile: ICAO database and Fuel Flow method II

The purpose of this work is to obtain an estimate of the emissions of pollutants as the parameters of a mission profile vary. The method used to base this estimate is the fuel flow method 2. For its correct application, however, it is necessary to know in advance the emissions values at sea level, in order to then be able to make a correction based on the change in altitude applied to the calculation of the fuel flow rate in the different flight conditions. For this purpose, the ICAO databank provides a valid source from which obtaining the emission values at zero altitude, however its limit lies in the unavailability of data relating to the use of non-traditional fuels. Consequently, following previous studies on the characteristics and performance of biofuels, a predictive estimate of the pollutants generated by them is made, thus expanding the availability of data contained in the ICAO database.

The application of the different methods together allows to obtain an estimate of the emission indexes for CO CO₂ NO_x and HC in the different phases of the mission profile, moment by moment, and finally an estimate of the total emissions during the entire flight envelope.

The calculation algorithm that summarizes the procedure followed to obtain the results discussed in the next chapter is presented below.

- 1) Obtaining corrective factors for EI_{sl} and $w_{f\ sl}$ resulting from the use of biofuels;
- 2) Expansion of the ICAO database with the inclusion of new types of fuel and corresponding performance characteristics;
- 3) Application of fuel flow method to obtain EI and w_f in different flight conditions;
- 4) Iteration of the fuel flow method to obtain emissions along the entire mission profile;

2.1 ICAO Annex 16: databank and LTO cycle prescriptions

The issue of the environmental impact of aircraft is included in Annex 16 of the Chicago Convention, which is in force in countries belonging to the ICAO – International Civil Aviation Organization. Mentioned ICAO Annex 16 contains 2 parts: the first concerns emissions and the second one is about aircraft noise. The emissions parts include the description of the methodology for assessing emission of harmful exhaust compounds from civil aircraft engines by universal LTO test (Landing and Take-off).²⁴

This test is a mapping of the operations carried out near the airports, i.e. taxiing, take off, climbing and approaching. For the case of civil aviation, the ICAO directives provide for a different thrust configuration for each phase:

- Take off $T=100\% T_{max}$
- Climb out $T=85\% T_{max}$
- Approach $T=30\% T_{max}$
- Taxi $T=7\% T_{max}$

The reference emissions LTO cycle for the calculation and reporting of gaseous emissions are represented by the following time in each operating mode. Phase Time in operating mode²⁵:

- Take off $t=0.7 \text{ min}$
- Climb out $t=2.2 \text{ min}$
- Approach $t=4 \text{ min}$
- Taxi $t=26 \text{ min}$

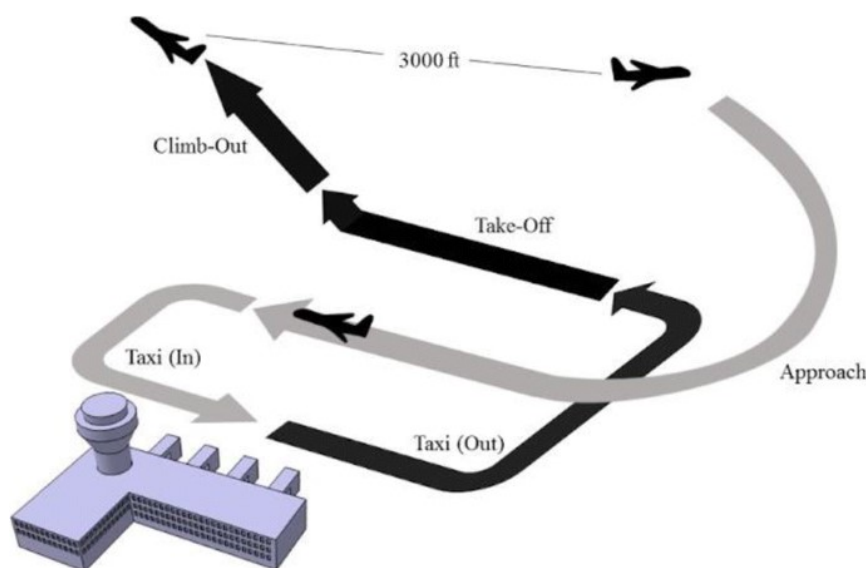


Figure 2.1 LTO cycle prescribed by ICAO in Annex 16 part II

²⁴ M. Nowak, R. Jasinski, M. Galant, *Implementation of the LTO cycle in flight conditions using FNPT II MCC simulator*, in IOP Conference series: materials science and engineering, pp 1-3

²⁵ Annex 16: Environmental protection, vol II: Aircraft Engine Emissions, 4th ed., ICAO

The emissions obtained according to the LTO test is defined as the mass of harmful compound per mass of fuel used in the test. It is expressed as the mass of compounds in 1g referred to 1000g of consumed fuel.

A generalized emission characterization for each single phase is presented in summary.

- Take off: the phase is characterized by the lower quantity of HC and CO, but at the same time by the maximum values of NO_x which are the result of the high temperatures in the combustion chamber;
- Climb: it differs slightly from the initial take off phase. In fact, the thrust is reduced by only 15%, as well as all the other performance parameters, slightly reduced. This guarantees a negligible variation in emissions;
- Approach and landing: emissions of carbon monoxide and unburnt hydrocarbons are higher than in the climb and take off phases due to the lower temperature of the combustion process;
- Taxi: the phase is characterized by a longer duration than the other phases and at the same time by the maximum values of HC and CO emitted. This makes this phase the most significant from the point of view of emissions within the entire LTO cycle;

Engine manufacturers generally carry out tests for certification and monitoring of polluting emissions by varying the performance of the same from minimum to maximum power, simulating the entire possible spectrum of flight regimes. However, the data obtained from these tests are not made public by the certification bodies and manufacturing companies, except in small quantities. Specifically, these are 4 characteristic points used in the calculations for obtaining the certification corresponding to the LTO duty cycle. These data are in practice those reported in the ICAO database. Although the inclusion in the data bank is entirely voluntary, most of the certified engines are present there, starting from 1982, the year in which the ICAO Emissions Standards were officially adopted.

So the International Civil Aviation Organization (ICAO) Engine Emissions Databank contains information, voluntarily provided by manufacturers, on exhaust emissions of production aircraft engines, measured according to the procedures in ICAO Annex 16 Vol II, and where noted, certified by their States of Design as implemented in their national regulations. This Databank contains information on only those engines that have entered production, irrespective of the numbers actually produced. It has been compiled mainly from information supplied for newly certified engines.

2.2 ICAO database correction

The data in the ICAO database, as anticipated, refer to tests conducted on engines fueled with traditional JET-A fuel. This work aims to analyze the emissions resulting from the use of biofuels. It is therefore necessary to make changes to the existing database, creating a parallel one referring to the new fuel class.

In the literature there are several studies on the performance characteristics of gas generators of aircraft engines. The results are presented below and refer to both the correction of the fuel flow and the correction of the emission indices.

2.2.1 Fuel Flow correction

A study by the University of Cranfield examined the effects of the variation in calorific value (heat capacity) and fuel density on the performance of the propulsion system in terms of thrust and fuel consumption²⁶. The influence of heat capacity and density was studied by simulating the use of a biofuel in a high bypass ratio turbofan using a tool / software developed in house called Pythia. Pythia is a software developed about 30 years ago by the University of Cranfield, capable of carrying out analyzes on the performance of aircraft engines of any type both in project conditions and in over-project conditions.

Two main types of biofuels were considered:

- Jatropa bio-synthetic paraffinic Kerosene, abbreviated JSPK, with molecular formula $C_{12}H_{26}$
- Camelina bio-synthetic paraffinic kerosene, abbreviated CSPK, with molecular formula $C_{12}H_{24.5}$,²⁷

In order to exploit the data obtained experimentally from this previous study, the analysis in its entirety will henceforth be developed with reference only to these two types of fuel.

²⁶ *Effects of biofuels properties on aircraft engine performance*, in *Aircraft Engineering and aerospace technology*, 87(5), pp 437-443, Emerald, 2013

²⁷ Muhammad Hanafi Azami, M. Savill, *Comparative study of alternative biofuels on aircraft engine performance*, in *Journal of Aerospace Engineering*, vol. 231, 2017, pp 1509-1521

Table 2.1 Biofuel properties

Properties	Jatropha	Camelina
Density [kg/m³]	864-880	780
Cetane number	46-55	50.4
Viscosity [mm²/s @40°C]	3.7-5.8	3.8
Pour Point [°C]	5	-7
Flash Point [°C]	163-238	136
Lower Heating Value [MJ/kg]	44.4	44
CFPP [°C]	-1.2	-3
Acid Value [mg/KOH]	0.34	-
Cloud Point [°C]	5	3
Oxidation Stability [h]	5	-
Iodine Value [I₂/100g]	109.5	152.8
Sulphur Content [ppm]	12.9	-
Specific Gravity [g/ml]	0.876	0.882
Molecular Formula	C ₁₂ H ₂₆	C ₁₂ H _{24.5}

The fuels considered were used both in pure form and in the form of a mixture in different percentages with traditional JET-A fuels, and to be exact in blends at 20, 40, 60, 80 and 100%. The purpose of the research is precisely to evaluate the effects and establish a relationship between the percentage of blend used and the performance of the propulsion system.

Tables 3.1 and 3.2 show the percentage variation in engine thrust, fuel consumption and SFC, calculated for the various biofuel blends (CSPK and JSPK respectively), comparing these values to those obtained through the use of traditional JET fuel. Specifically, compared to JET-A, both biofuels show an increase in thrust and fuel flow, but a reduction in the SFC, despite the latter being negligible.

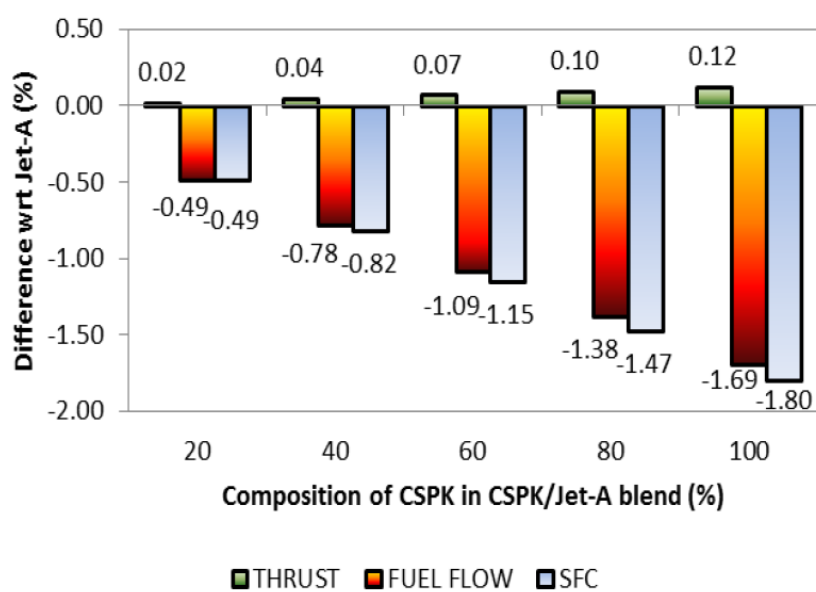
The data obtained from this study were used to obtain a corrective coefficient to be applied for the correction of the fuel flow in the ICAO database tables, as, as is well known, this makes available only and exclusively data obtained from experimental tests on aero engines powered by JET-A. It is therefore assumed that the performance or behavior of each engine broadly reflects that of the model used for the simulation using the PYTHIA software.

Table 2.2 Thrust, fuel flow and sfc for different blend of CSPK

BLEND	THRUST	FUEL FLOW	SFC
20%	0.02	-0.49	-0.49
40%	0.04	-0.78	-0.82
60%	0.07	-1.09	-1.15
80%	0.1	-1.38	-1.47
100%	0.12	-1.69	-1.8

Table 2.3 Thrust, fuel flow and sfc for different blend of JSPK

BLEND	THRUST	FUEL FLOW	SFC
20%	0.01	-0.6	-0.61
40%	0.03	-1.03	-1.05
60%	0.05	-1.46	-1.5
80%	0.07	-1.88	-1.94
100%	0.09	-2.31	-2.39

**Figure 2.2** Thrust, fuel flow and sfc for different blend of CSPK

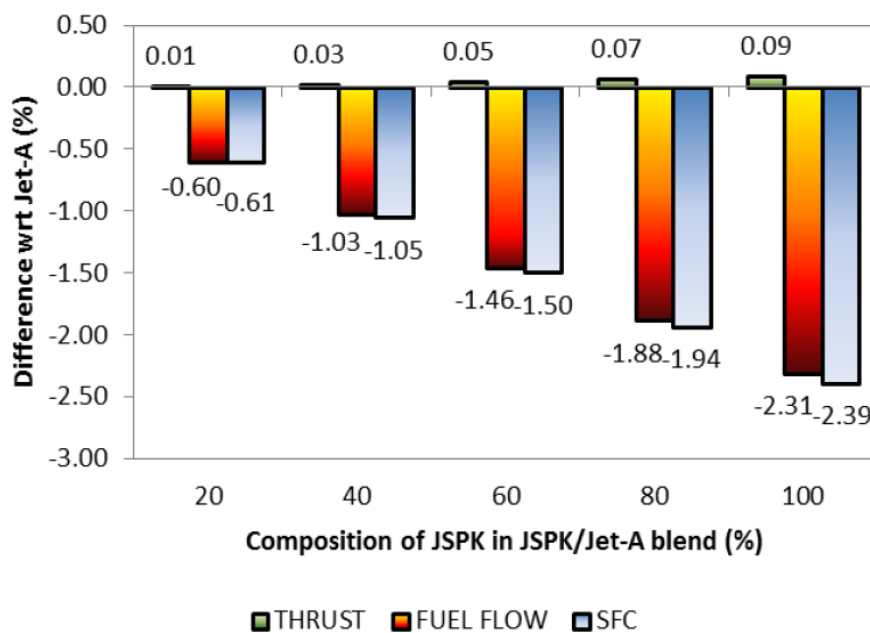


Figure 2.3 Thrust, fuel flow and sfc for different blend of JSPK

Once the corrective factors have been obtained to be able to modify the fuel flow made available in the ICAO database, which we recall refers only and exclusively to the combustion of Jet-A1 fuel, it is necessary to find a method to calculate the emissions of pollutants, and specifically of CO, NO_x and HC, in relation to the use of biofuels.

As previously mentioned in this research it was decided to analyze only HEFA CSPK and JSPK fuels.

2.2.2 Emission index correction

B. Gawron, T. Bialecki et al.²⁸ estimate the emissions resulting from the use of biofuels.

Specifically, reference is made to HEFA CAM and UCO. CAM stands for Camelina, so it is the equivalent of the CSPK; as for the UCO EFAs, on the other hand, they are biofuels obtained from cooking oil. It was therefore necessary at this point to compare the properties of the latter with those of the JSPK, in order to justify the replacement within the analysis. The data obtained shows a remarkable similarity between the two categories of biofuels, in terms of density, combustion efficiency and lower heating value, which is why it was considered appropriate to exploit the data obtained experimentally from the combustion of UCO, assuming similar characteristics and results for the JSPK.

The study derived percentage corrective factors to be applied to the data already present related to the use of traditional fuel. The discussion neglects the variation of unburned hydrocarbons, which is why their value will be kept constant during the subsequent analysis. Each simulation of the aforementioned study, aimed at obtaining the emission indices, is carried out at different rotational speed values of the engine, each related to the different thrust configurations characteristic of each phase of the LTO cycle. As the rotational speed and consequently the thrust of the engine increase, it is evident how the emissions of carbon monoxide are reduced, while the emissions of nitrogen oxides and carbon dioxide are increasing.

Tables 3.4 and 3.5 summarize the research results that will be applied in order to create an extension of the ICAO database for CSPK and JSPK biofuel cases

Table 2.4 Emission index CO correction [%]

	IDLE	APPROACH	CRUISE	TAKEOFF
CSPK 50%	-6	-8.5	-0.5	11
CSPK 20%	-2.4	-3.4	-0.2	4.4
CSPK 40%	-4.8	-6.78	-0.4	8.8
CSPK 60%	-7.2	-10.2	-0.6	13.2
CSPK 80%	-9.6	-13.6	-0.8	17.6
CSPK 100%	-12	-17	-1	22
JSPK 50%	-4	-7	-6	0.2
JSPK 20%	-1.6	-2.8	-2.4	0.08

²⁸B. Gawron, T. Bialecki, A. Janicka, T. Suchocki, *Combustion and Emissions Characteristics of the turbine engine fueled with HEFA Blends from different feedstock*, in *Energies*, vol. 1277, 2020, pp 1-12

JSPK 40%	-3.2	-5.6	-4.8	0.16
JSPK 60%	-4.8	-8.4	-7.2	0.24
JSPK 80%	-6.4	-11.2	-9.6	0.32
JSPK 100%	-8	-14	-12	0.4

Table 2.5 Emission index Nox correction [%]

	IDLE	APPROACH	CRUISE	TAKEOFF
CSPK 50%	21.8	17.5	15	10.5
CSPK 20%	8.72	7	6	4.2
CSPK 40%	17.44	14	12	8.4
CSPK 60%	26.16	21	18	12.6
CSPK 80%	34.88	28	24	16.8
CSPK 100%	43.6	35	30	21
JSPK 50%	11.5	9.5	7.9	4.9
JSPK 20%	4.6	3.8	3.16	1.96
JSPK 40%	9.2	7.6	6.32	3.92
JSPK 60%	13.8	11.4	9.48	5.88
JSPK 80%	18.4	15.2	12.64	7.84
JSPK 100%	23	19	15.8	9.8

2.2.3 CO₂ emissions calculation method

In the ICAO database there are no references regarding the production and emissions of carbon dioxide. For this reason it was necessary to find in the literature a method suitable for calculating the aforementioned emissions.

For this purpose it was assumed to use the COPERT model²⁹. This estimates the emissions generated by road transport and internal combustion engines. Although this model may seem inappropriate at first sight, it differentiates between types of pollutants, which allows us to exploit it even in the aeronautical case in the case of carbon dioxide emissions.

The model of calculating the exhaust emissions differs on the basis of the identification of four groups of pollutants:

- Group 1: CO, NO_x, COV, CH₄, COVNM, N₂O, NH₃ e PM. For these pollutants, specific emission factors linked to the different conditions of the engine and to the operating cycles are used;
- Group 2: CO₂, SO₂. The emissions of these pollutants are estimated solely on the basis of fuel consumption;
- Group 3: IPA, PCDD e POP. On these pollutants no detailed data is available and a simplified methodology is used;
- Group 4: pollutants obtained as a fraction of total NMVOC emissions;

Obviously, the group of interest for the purposes of this request is Group 2, which makes it possible to estimate CO₂ emissions. And, as previously mentioned, although this refers to a model developed for road transport, it can also be used on an aeronautical model as it is based solely and exclusively on the combustion process, on the molecular characteristics of the fuel and on its consumption.

So for the purposes of calculating CO₂ emissions, it is assumed that the carbon content of the fuel is oxidized to 99% into CO₂. If the composition of the fuel is known, denoting by c, h and o the mass fractions of the carbon, hydrogen and oxygen atoms, with c+h+o=1, the ratios between hydrogen and carbon and between oxygen and carbon in the fuel are respectively equal to:

$$r_{H:C} = 11.916 \frac{h}{c} \quad (2.1)$$

$$r_{O:C} = 0.7507 \frac{o}{c} \quad (2.2)$$

²⁹ A. Bernetti, R. De Lauretis, G. Iarocci, F. Lena, R. Marra Campanale, E. Taurino, *Inventario nazionale delle emissioni e disaggregazione provinciale*, Istituto Superiore per la Ricerca e Protezione Ambientale, 2010

The calculation of CO₂ emissions from aircraft powered by fuel k and equipped with technology t is obtained from:

$$E_{CO_2,t,k}^{CALC} = 44.011 \frac{FC_{t,k}^{CALC}}{12.011 + 1.008 r_{H:C,t} + 16 r_{O:C,t}} \quad (2.3)$$

where $FC_{t,k}^{CALC}$ corresponds to the fuel consumption k for the technology under consideration t.

For the purpose of estimating the final exhaust emissions, other emissions of carbon atoms are also considered, such as, with reference to technology t and fuel k, emissions of carbon monoxide CO:

$$E_{CO_2,t,k}^{CALC} = 44.011 \left(\frac{FC_{t,k}^{CALC}}{12.011 + 1.008 r_{H:C,t} + 16 r_{O:C,t}} - \frac{E_{t,k}^{CO}}{28.011} \right) \quad (2.4)$$

It is therefore necessary to take into account the molecular structure of the fuels under consideration, namely JET-A, JSPK and CSPK.

2.3 Obtaining characteristics curves

Table 3.6 shows part of the database thus obtained. Specifically, it was decided to report the performance characteristics to varying the type of fuel for a single type of engine, purely by way of example (CFM International CFM56-5A4). Regardless of this, obtaining the emission values and fuel flow rates for each individual phase of the cycle, allows to obtain characteristic curves (Fig. 3.4), which will be exploited in the subsequent part of the analysis.

The data will be interpolated through the values obtained from the fuel flow, allowing the analysis of emissions at high altitude. By exploiting the a priori knowledge of the relationship between EI and fuel flow in the different flight phases, thanks to the data obtained from the ICAO database, it is possible to represent first degree curves.

By way of example, the graph obtained using the characteristics of the CFM56-5A4 engine powered by traditional Jet fuel for the purposes of the simulation is shown. As mentioned previously, CO and HC have a maximum value in the taxi phase and a decreasing trend with increasing fuel flow. Conversely, opposite behavior for CO₂ and NO_x.

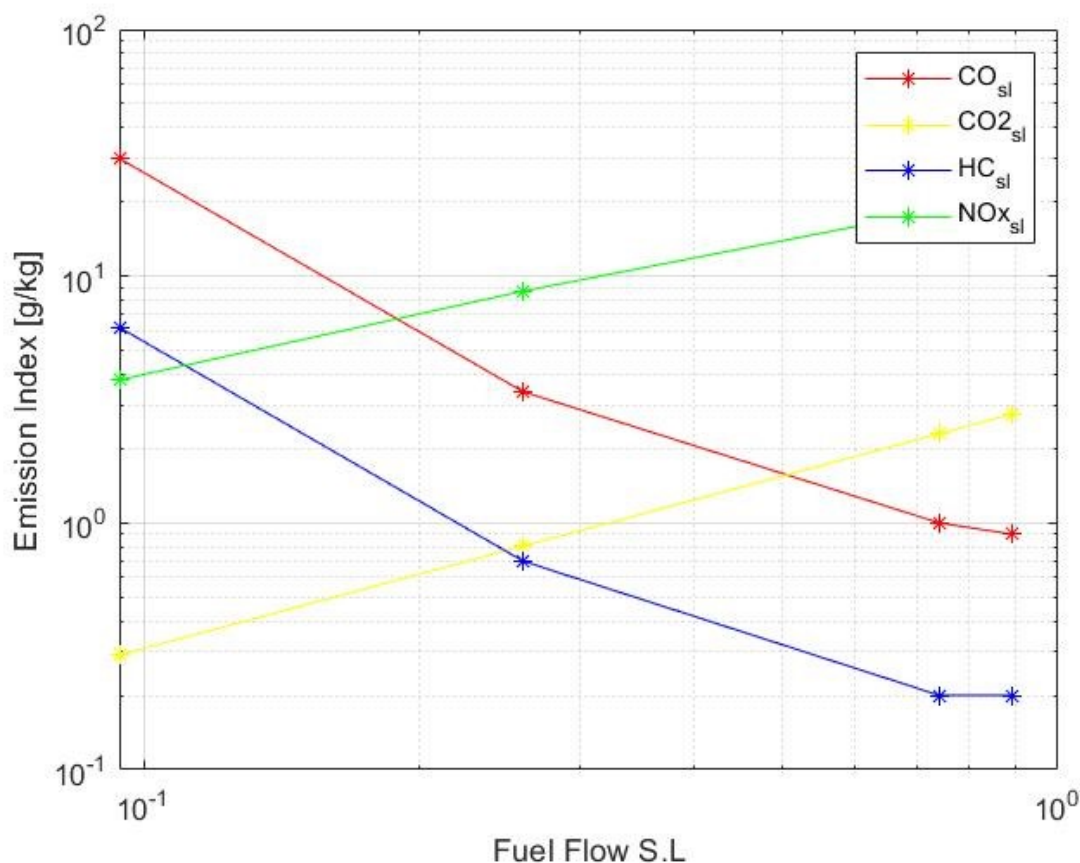


Figure 2.4 Emissions characteristic curve CFM56-5A4 using JET-A

Table 2.6 Emission index for CFM International CFM56-5A4 (Airbus A-320), for different type of fuel

Fuel	JET A1	CSPK 20%	CSPK 40%	CSPK 60%	CSPK 80%	CSPK 100%	JSPK 20%	JSPK 40%	JSPK 60%	JSPK 80%	JSPK 100%
Rated Thrust (kN)	97.89	97.89	97.89	97.89	97.89	97.89	97.89	97.89	97.89	97.89	97.89
HC EI T/O (g/kg)	0.23	0.23	0.23	0.23	0.23	0.23	0.23	0.23	0.23	0.23	0.23
HC EI C/O (g/kg)	0.23	0.23	0.23	0.23	0.23	0.23	0.23	0.23	0.23	0.23	0.23
HC EI App (g/kg)	0.5	0.5	0.5	0.5	0.5	0.5	0.5	0.5	0.5	0.5	0.5
HC EI Idle (g/kg)	1.75	1.75	1.75	1.75	1.75	1.75	1.75	1.75	1.75	1.75	1.75
CO ₂ T/O kg/s	2.7807	2.7999	2.7918	2.7831	2.7749	2.7662	2.7969	2.7848	2.7727	2.7609	2.7488
CO ₂ C/O kg/s	2.294	2.3099	2.3032	2.296	2.2892	2.282	2.3073	2.2974	2.2874	2.2776	2.2676
CO ₂ App kg/s	0.8091	0.7147	0.8123	0.8098	0.8074	0.8049	0.8138	0.8103	0.8068	0.8033	0.7998
CO ₂ Idle kg/s	0.2945	0.2965	0.2957	0.2947	0.2939	0.293	0.2962	0.2949	0.2937	0.2924	0.2911
CO EI T/O (g/kg)	1.1	1.1484	1.1968	1.2452	1.2936	1.342	1.0088	1.1018	1.1026	1.1035	1.1044
CO EI C/O (g/kg)	1.1	1.0978	1.0956	1.0934	1.0912	1.089	1.0736	1.0472	1.0208	0.9944	0.968
CO EI App (g/kg)	3.1	2.9946	2.8892	2.7838	2.6784	2.573	3.0132	2.9326	2.8396	2.7528	2.666
CO EI Idle (g/kg)	20.3	19.8128	19.3256	18.8384	18.3512	17.864	19.9752	19.6504	19.3256	19.0008	18.676
NO _x EI T/O (g/kg)	22.64	23.5909	24.5418	25.4926	26.4435	27.3944	23.0837	23.5275	23.9712	24.415	24.8587
NO _x EI C/O (g/kg)	19.11	20.2566	21.4032	22.5498	23.6964	24.843	19.7139	20.3178	20.9216	21.5255	22.1294
NO _x EI App (g/kg)	8.51	9.1057	9.7014	10.2971	10.8928	11.4885	8.8334	9.1568	9.4801	9.8035	10.1269
NO _x EI Idle (g/kg)	4.04	4.3923	4.7446	5.0969	5.4492	5.8014	4.2258	4.4117	4.5975	4.7834	4.9692
Fuel Flow T/O (kg/sec)	0.897	0.8926	0.89	0.8872	0.8846	0.8818	0.8916	0.8878	0.8839	0.8801	0.8763
Fuel Flow C/O (kg/sec)	0.74	0.7364	0.7342	0.7319	0.7298	0.7275	0.7356	0.7324	0.7292	0.7261	0.7229
Fuel Flow App (kg/sec)	0.261	0.2597	0.259	0.2582	0.2574	0.2566	0.2594	0.2583	0.2572	0.2561	0.2549
Fuel Flow Idle (kg/sec)	0.095	0.0945	0.0943	0.094	0.0936	0.0933	0.0944	0.094	0.0936	0.0932	0.0928
Ambient Baro Min (kPa)	94.7	94.7	94.7	94.7	94.7	94.7	94.7	94.7	94.7	94.7	94.7
Ambient Baro Max (kPa)	95.6	95.6	95.6	95.6	95.6	95.6	95.6	95.6	95.6	95.6	95.6
Ambient Temp Min (K)	280	280	280	280	280	280	280	280	280	280	280
Ambient Temp Max (K)	291	291	291	291	291	291	291	291	291	291	291
Humidity Min (kg/kg)	0.0026	0.0026	0.0026	0.0026	0.0026	0.0026	0.0026	0.0026	0.026	0.026	0.026
Humidity Max (kg/kg)	0.0034	0.0034	0.0034	0.0034	0.0034	0.0034	0.0034	0.0034	0.0034	0.034	0.034

As previously said about the ICAO regulations, it is possible to obtain the emission trend during an entire LTO cycle by considering not only the values present in the database but also the

requirements regarding the duration of each individual phase. The following pages show the graphs relating to emissions of CO (fig. 3.5), CO₂ (fig. 3.6), HC (fig. 3.7), and Nox (fig. 3.8).

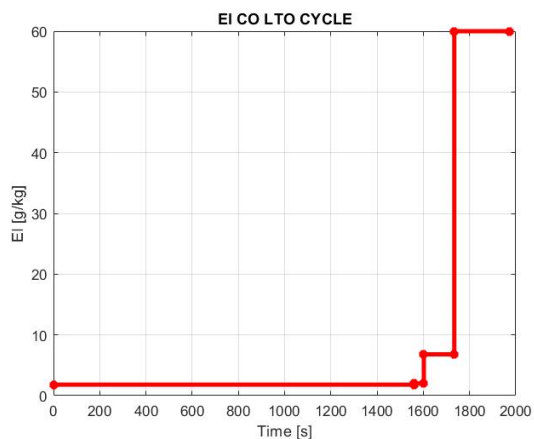


Figure 2.5 EICO LTO cycle for CFM56-5°4

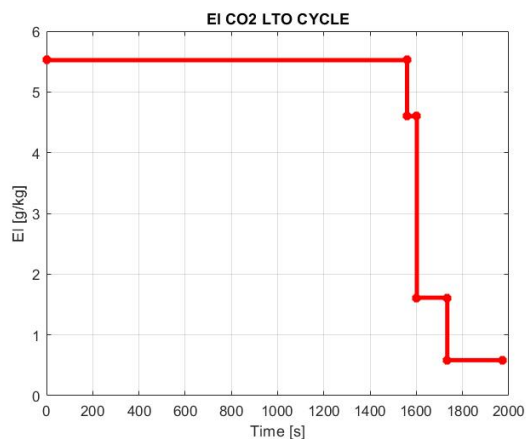


Figure 2.6 EICO2 LTO cycle for CFM56-5°4

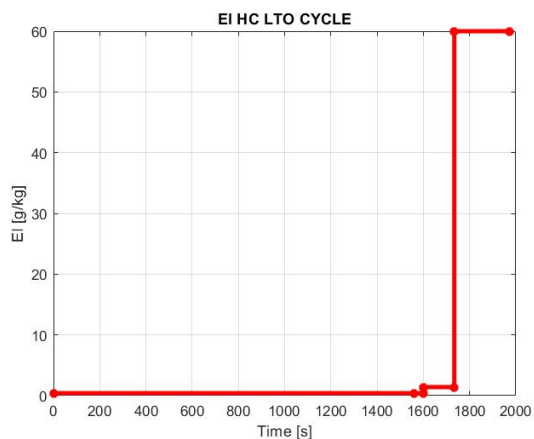


Figure 2.7 EIHC LTO cycle for CFM56-5°4

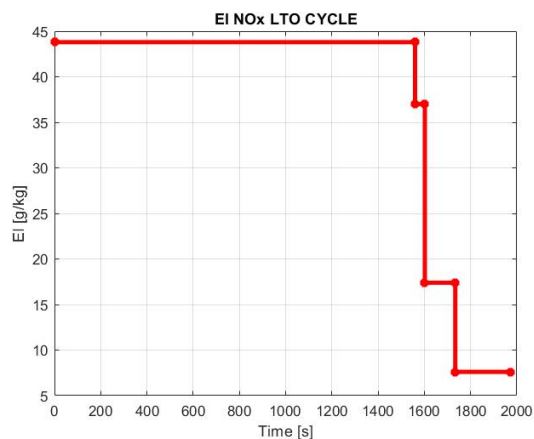


Figure 2.8 EINOx LTO cycle for CFM56-5°4

2.4 Fuel flow method 2

At this point, after having obtained the emission indices relating to a standard LTO cycle, a method must be adopted that guarantees the possibility of carrying out the assessment as flight conditions vary, thus allowing to obtain an estimate of the emissions of pollutants while cruising, at high altitude and in general along an entire mission profile. For this purpose, the Fuel Flow Method 2 is used³⁰.

The recent scenarios, discussed extensively in the previous chapters, have led to the aeronautical sector the need to quantify the emissions generated by aeroengines. The main and best known method in the sector for the calculation of NO_x HC and CO is the so-called "P3T3".

Although not as rigorous as the P3T3, the Fuel Flow Method represents a valid alternative for emissions certification. This method can offer an approximation of the emissions with nominal calculated values characterized by an error of 10-15% compared to those obtained with the traditional P3T3.

The P3T3 requires knowledge of the evolution of the parameters inside the engine, and in particular through the high pressure compressor and the combustor diffuser. The parameters under consideration are the total pressure p_3 (in this treatment p_2), and the total temperature T_3 (in this treatment T_2), the input parameters in the combustor, the fuel flow rate w_f . Furthermore, for the sole purpose of calculating the emissions of nitrogen oxides, it is also necessary to know the relative humidity of the environment. This information is then fed into a model that evaluates the performance of the machine. It is evident that not all the information necessary to carry out the analysis using the P3T3 method can be easily found, and some of them can only be obtained through the proprietary performance model. As a consequence of this, methods with a simplified approach have been proposed, based solely on the dependence on the flow rate of fuel in the combustion chamber w_f such as fuel flow. However, for the correct application of the latter, knowledge of the typical emission indices of the LTO cycle is required, usually provided after the ICAO certification process.

The method used is presented below, and is divided into two fundamental parts: the first aims to obtain a correction of the emission indices as the altitude varies, the second instead is useful for obtaining a relationship that allows to correct the value of fuel flow with altitude.

³⁰ D. Dubois, G. C. Paynter, Fuel Flow Method 2 for estimating Aircraft emissions, The Boeing Company, SAE international, 2006

2.4.1 Emission index correction with altitude

It is assumed that the compression process between the combustor inlet and the air intake is isentropic:

$$\frac{T_2}{T_1} = \left(\frac{p_2}{p_1}\right)^{\frac{\gamma-1}{\gamma}} \quad (2.5)$$

$$T_2 = T_1 \left(\frac{p_2}{p_1}\right)^{\frac{\gamma-1}{\gamma}} \quad (2.6)$$

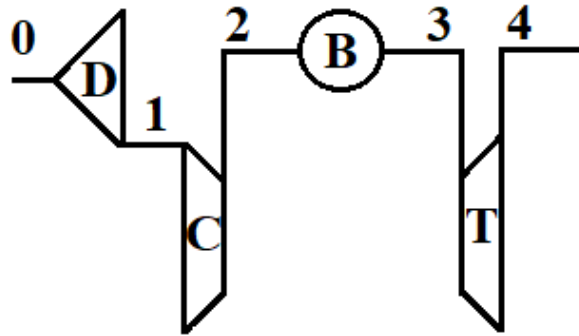


Figure 2.94 Gas generator scheme

Writing the equation to the flight conditions:

$$T_{2 \text{ alt}} = T_{1 \text{ alt}} \left(\frac{p_{2 \text{ alt}}}{p_{1 \text{ alt}}}\right)^{\frac{\gamma-1}{\gamma}} \quad (2.7)$$

and at seal level

$$T_{2 \text{ sl}} = 518.67 \left(\frac{p_{2 \text{ sl}}}{14.696}\right)^{\frac{\gamma-1}{\gamma}} \quad (2.8)$$

Furthermore it can be assumed that

$$T_{2 \text{ sl}} = T_{2 \text{ alt}} \quad (2.9)$$

Taking advantage of this last relationship, and joining it to the previous ones, we obtain:

$$T_{1\ alt} \left(\frac{p_{2\ alt}}{p_{1\ alt}} \right)^{\frac{\gamma-1}{\gamma}} = 518.67 \left(\frac{p_{2\ sl}}{14.696} \right)^{\frac{\gamma-1}{\gamma}} \quad (2.10)$$

Which can be rewritten as

$$\frac{p_{2\ alt}}{p_{2\ sl}} = \frac{\delta_1}{\theta_1^{\frac{\gamma-1}{\gamma}}} \quad (2.11)$$

A beta coefficient is now introduced which takes into account the ratio between total and static quantities, such that

$$\beta = 1 + \frac{\gamma-1}{2} M^2 \quad (2.12)$$

You can then write that

$$\frac{p_{2\ alt}}{p_{2\ sl}} = \frac{\delta_{amb} \beta^{\frac{\gamma}{\gamma-1}}}{(\theta_{amb} \beta)^{\frac{\gamma}{\gamma-1}}} = \frac{\delta_{amb}}{\theta_{amb}^{\frac{\gamma}{\gamma-1}}} \quad (2.13)$$

And considering $\gamma=1.4$ for air

$$\frac{p_{2\ alt}}{p_{2\ sl}} = \frac{\delta_{amb}}{\theta_{amb}^{1.5}} \quad (2.14)$$

If a polytropic efficiency is used to describe the compression between sections 2 of the combustor inlet and 1 of the air intake, then the relationship between pressures and temperatures becomes

$$\frac{T_2}{T_1} = \left(\frac{p_2}{p_1} \right)^{\frac{\gamma-1}{\eta_p \gamma}} \quad (2.15)$$

And considering $\gamma=1.38$ e $\eta_p = 90\%$

$$\frac{p_{2\ alt}}{p_{2\ sl}} = \frac{\delta_{amb}}{\theta_{amb}^{1.3}} \quad (2.16)$$

A small further empirical correction is then made

$$\frac{p_{2\ alt}}{p_{2\ sl}} = \frac{\delta_{amb}^{1.02}}{\theta_{amb}^{1.3}} \quad (2.17)$$

Substituting this result in the equations of the P3T3 model, we obtain:

$$EICO_{alt} = EICO_{sl} \left(\frac{\theta_{amb}^{3.3}}{\delta_{amb}^{1.02}} \right)^x \quad (2.18)$$

$$EIH C_{alt} = EIH C_{sl} \left(\frac{\theta_{amb}^{3.3}}{\delta_{amb}^{1.02}} \right)^x \quad (2.19)$$

$$EINO x_{alt} = EINO x_{sl} \left(\frac{\theta_{amb}^{3.3}}{\delta_{amb}^{1.02}} \right)^x \quad (2.20)$$

The exponents x and y , in the absence of further indications, are usually set at 1 and 0.5 respectively.

2.4.2 Fuel flow correction with altitude

By writing the energy balance equation to the combustor, a corrective factor for the fuel flow rate can be obtained

$$\eta_b w_f LHV = (w_f + w_a) C_p (T_3 - T_2) \quad (2.21)$$

Since the fuel flow is typically less than 2% of the total air flow, and furthermore if both the air flow and the fuel flow are assumed to be at the same temperature, i.e. T_2 , and have the same heat specific, a simplification can be made and the equation can be rewritten as

$$\eta_b w_f LHV = w_a C_p (T_3 - T_2) \quad (2.22)$$

Applying this equation at altitude and at sea level, and assuming that the temperatures T_3 and T_2 remain unchanged with the altitude

$$w_{f\ sl} = w_{f\ alt} \frac{w_{a\ sl} \eta_{b\ alt}}{w_{a\ alt} \eta_{b\ sl}} \quad (2.23)$$

The air flow in the combustor at sea level can be written as

$$w_{a\ sl} = k \frac{p_{2\ sl}}{\sqrt{T_{2\ sl}}} f(M_2)_{sl} \quad (2.24)$$

where

$$k = \frac{\sqrt{\gamma}}{\sqrt{R T_3}} \quad (2.25)$$

And the Mach function takes the form

$$f(M_3)_{sl} = M \left(\frac{1}{\frac{\gamma-1}{2} M^2 + 1} \right)^{\frac{\gamma+1}{2(\gamma-1)}} \quad (2.26)$$

A similar expression can be written for conditions at defined altitude

$$w_{a\ alt} = k \frac{p_{2\ alt}}{\sqrt{T_{2\ alt}}} f(M_2)_{alt} \quad (2.27)$$

Furthermore, since the output of the combustor is choked and the total temperatures at the entrance and exit of the same are considered equal at zero altitude and cruising, it can be assumed that

$$f(M_2)_{sl} \approx f(M_2)_{alt} \quad (2.28)$$

By substituting the expressions found for the air flow within the equation obtained for the energy balance, we obtain

$$w_{f\ sl} = w_{f\ alt} \frac{p_{2\ sl}}{p_{2\ alt}} \frac{\eta_{b\ alt}}{\eta_{b\ sl}} \quad (2.29)$$

The efficiency of the combustor can be rewritten by always referring to the energy balance equation

$$\eta_b = \frac{k}{\frac{w_f}{w_a}} \quad (2.30)$$

where

$$k = C_p(T_3 - T_2)/LHV \quad (2.31)$$

And by replacing it again, an expression is obtained for the correction of the fuel flow rate with the altitude that does not take into account the efficiency of the burner,

$$w_{f\ sl} = w_{f\ alt} \frac{p_{2\ sl}}{p_{2\ alt}} \frac{(\frac{w_f}{w_a})_{sl}}{(\frac{w_f}{w_a})_{alt}} \quad (2.32)$$

Referring to Eq. 3.15, obtained previously,

$$\frac{p_{2\ sl}}{p_{2\ alt}} = \frac{\theta_{amb}^{1.5}}{\delta_{amb}} \quad (2.33)$$

And replacing it in eq. 3.32

$$w_{f\ sl} = w_{f\ alt} \frac{\theta_{amb}^{1.5}}{\delta_{amb}} \frac{(\frac{w_f}{w_a})_{sl}}{(\frac{w_f}{w_a})_{alt}} \quad (2.34)$$

At this point, a relationship between the fuel air dilution ratio and the inlet temperature to the combustor can be introduced, using the non-dimensional parameters of the analysis

$$T_{2\,sl} = \frac{T_{2\,alt}}{\theta_1} \quad (2.35)$$

$$\left(\frac{w_f}{w_a}\right)_{sl} = \frac{\left(\frac{w_f}{w_a}\right)_{alt}}{\theta_1} \quad (2.36)$$

Then is introduced a corrective factork ,assumed constant,

$$\frac{\left(\frac{w_f}{w_a}\right)_{alt}}{\theta_1} = k \left(\frac{T_{2\,sl}}{\theta_1}\right)^x \quad (2.37)$$

This last equation can also be rewritten at sea level,

$$\left(\frac{w_f}{w_a}\right)_{alt} = k (T_{2\,sl})^x \quad (2.38)$$

And comparing the two relations (at altitude and at sea level), again considering the constant T3 as the altitude varies,

$$\left(\frac{w_f}{w_a}\right)_{sl} = \left(\frac{w_f}{w_a}\right)_{alt} \theta_1^{x-1} \quad (2.39)$$

Now, replacing the equation obtained within the relationship for calculating the fuel flow rate at sea level (eq. 3.34)

$$w_{f\,sl} = w_{f\,alt} \frac{\theta_{amb}^{3.5}}{\delta_{amb}} \theta_1^{x-1} \quad (2.40)$$

From experimental data the exponent x is fixed equal to 2 and consequently it is obtained:

$$w_{f\,sl} = w_{f\,alt} \frac{\theta_{amb}^{3.5}}{\delta_{amb}} \theta_1 \quad (2.41)$$

Considering then compressible flow function relationships fot total to static pressure and temperature,

$$\theta_1 = \theta_{amb} \left(1 + \frac{\gamma - 1}{2} M^2\right) \quad (2.42)$$

Replacing θ_1 , and $\gamma=1.4$, eq. 3.41 will be

$$w_{f\,sl} = w_{f\,alt} \frac{\theta_{amb}^{3.5}}{\delta_{amb}} \theta_{amb} (1 + .2M^2) \quad (2.43)$$

From perturbation theory,

$$e^{0.2M^2} \approx (1 + .2M^2) \quad (2.44)$$

We can therefore write that

$$w_{f\ sl} = w_{f\ alt} \frac{\theta_{amb}^{4.5}}{\delta_{amb}} e^{0.2M^2} \quad (2.45)$$

$$w_{f\ sl} = w_{f\ alt} \frac{\theta_{amb}^{3.8}}{\delta_{amb}} e^{0.2M^2} \quad (2.46)$$

2.4.3 Data interpolation and mission analysis

The fuel flow allows first of all to obtain the fuel flow rate above sea level (eq. 3.46) knowing the fuel flow rate at altitude. This relationship, together with the characteristic curves of paragraph 3.4, will make it possible to calculate, by interpolation, the corresponding emissions referring to sea level. Subsequently, thanks to relations 2.18, 2.19 and 2.20, it will be possible to obtain the final result, that is the emissions of pollutants in the different flight conditions, different from those of the LTO cycle.

Again by way of example, and referring to the previously reported case of the CFM56-5A4 engine, a complete analysis of the emissions along the typical mission profile of an Airbus A320 is provided below, which is summarized in the table, together with the parameters entered in input and required to perform the calculation. The code used to carry out the simulations is contained in Appendix A, and consists of a series of iterative calculations, which instant by instant calculate the emissions of compounds as the flight conditions vary by interpolating the characteristic curves obtained from the database and the corrections presented above. Figure 2.10 shows a summary diagram of the calculation algorithm, highlighting inputs, outputs and processes.

Table 2.7 Input parameters for mission profile simulation

	IDLE	TAKE OFF	CLIMB	CRUISE	APPROACH	LANDING
Max speed (M)	0.05	0.23	0.5	0.7	0.4	0.2
Max altitude [m]	0	1000	10000	10000	10000	1000
Min altitude [m]	0	0	1000	10000	1000	0
Time [s]	1200	60	120	3600	600	120
Fuel flow [kg/s]	0.01	0.9	0.7	0.5	0.3	0.2

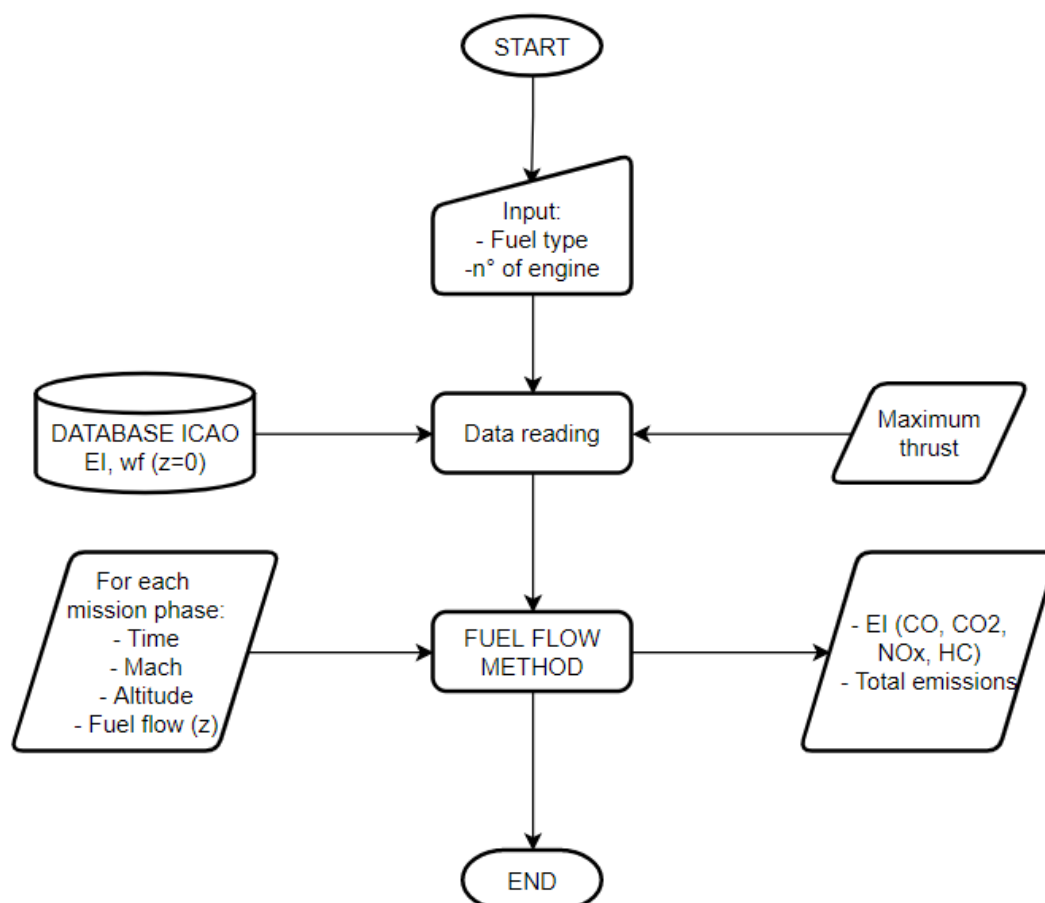


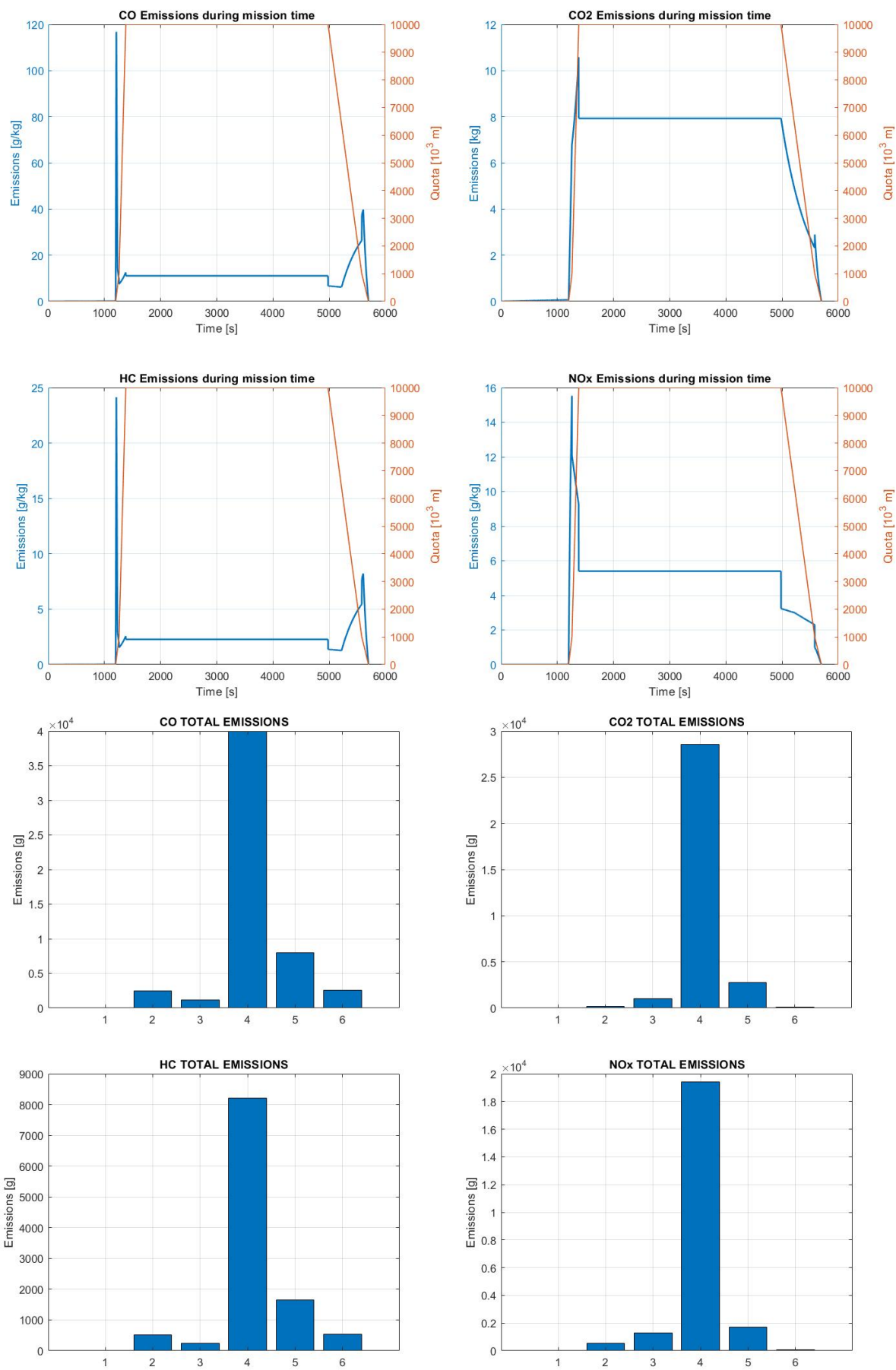
Figure 2.10 Flow chart of the algorithm used to develop matlab code for emissions calculations

Three different simulations are then carried out in order to highlight the difference relating to the use of different types of fuels. The first case sees the use of JET-A1, the second CSPK and the third JSPK.

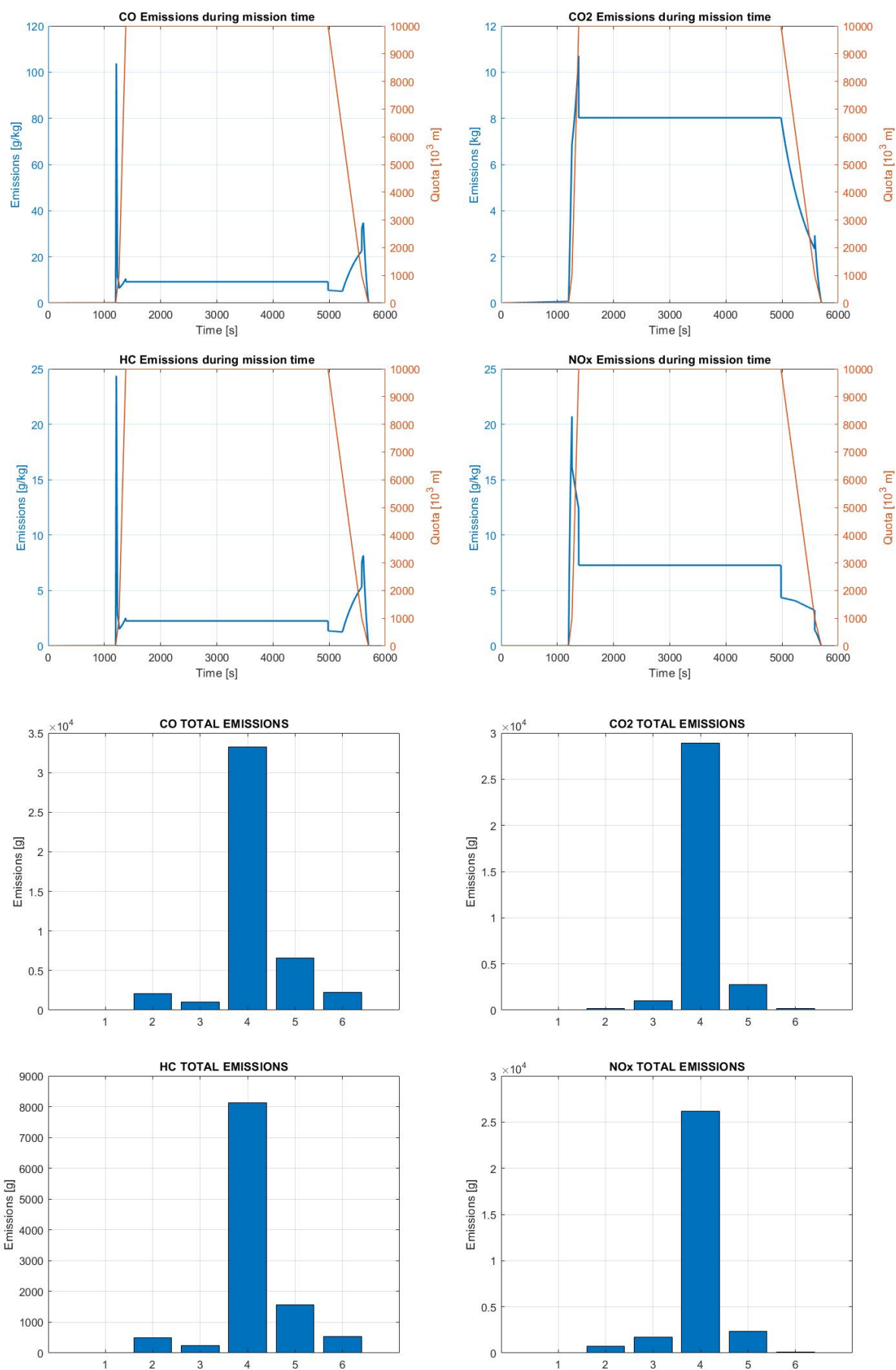
In the initial phase, a twin-engine configuration is set with a maximum thrust of the aircraft equal to 200 kN; the results presented subsequently will therefore not refer to the performance of the single engine, but to the entire propulsion system, thus representing a complete analysis of the emissions generated by a short-haul flight (1.5 hours of operating cycle).

N.B in the histograms on the following pages: 1=taxi, 2=takeoff, 3=climb, 4=cruise, 5=approach, 6=landing.

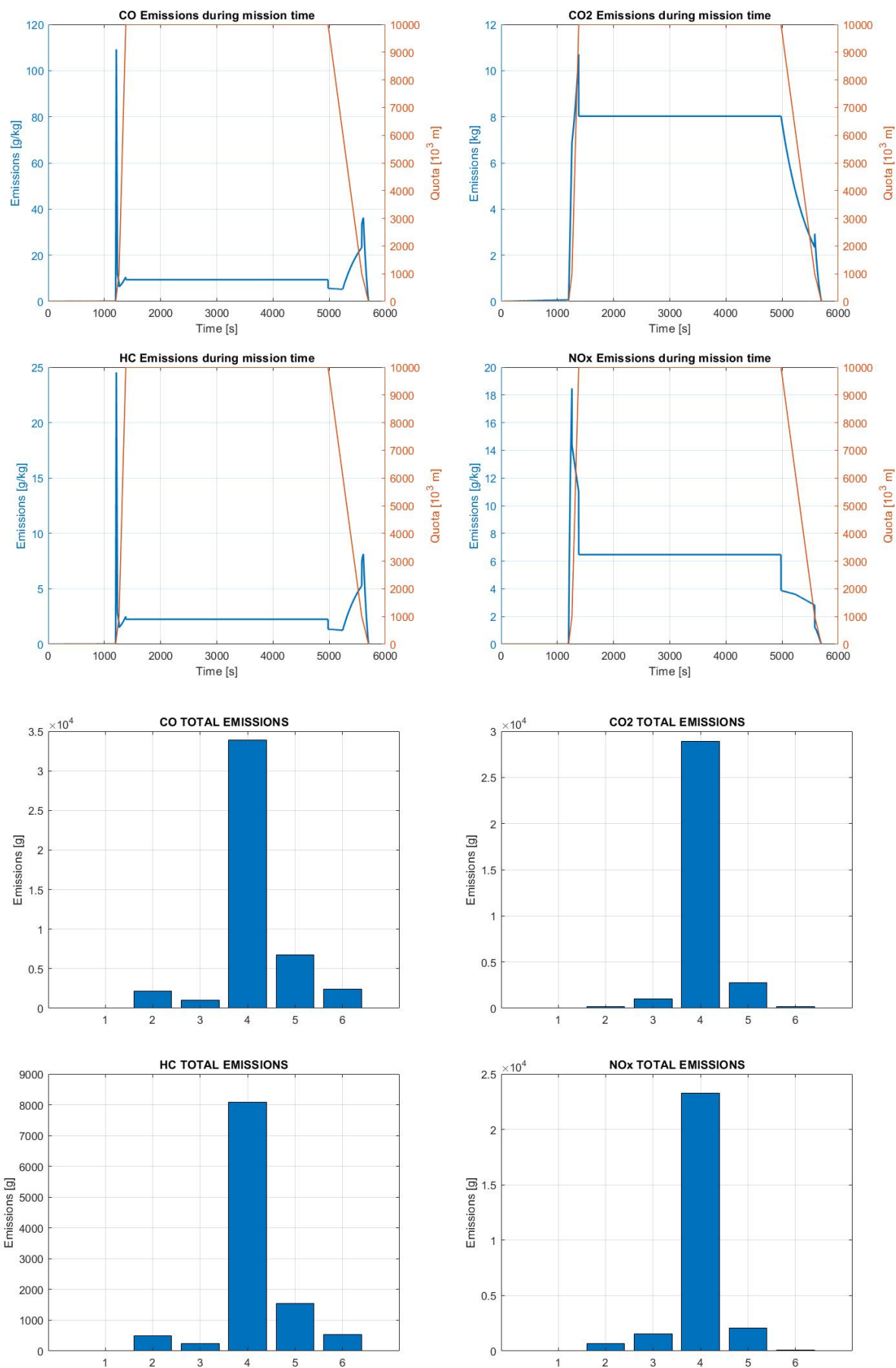
2.4.3.1 JET-A1



2.4.3.2 CSPK (100%)

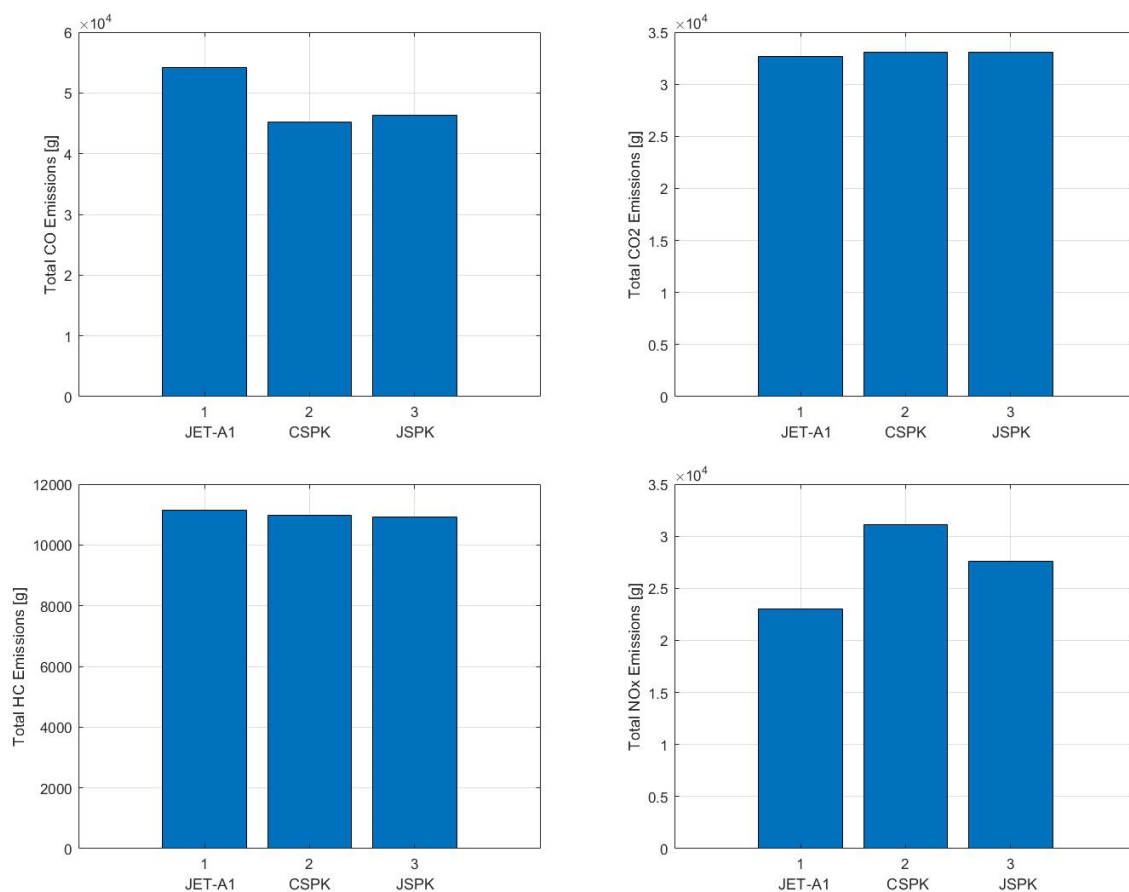


2.4.3.3 JSPK (100%)



2.4.3.4 Results and Discussion

It is evident that in the cases analyzed the greatest contribution of pollutants is to be attributed to the cruise phase. This is not so much linked to the performance characteristics of the aircraft, as to the time set for the aforementioned phase; for the simulation a time of 3600 sec has been set (1h) for the cruise only, while all the other phases are typically of shorter duration. By focusing on the total quantities of pollutants generated by the combustion of the three different types of fuels, comparing kerosene and biofuels, for the latter it is possible to observe a substantial reduction in the emissions of carbon dioxide, unburnt hydrocarbons and an increase nitrogen oxides, while it is a slight increase in the generation of carbon dioxide (albeit negligible) is noticeable. Nevertheless, the advantage of using biofuels lies not so much in the CO₂ limitations related to its practical use as an oxidizer, as in the entire extraction and production cycle, as widely described in chapter 1. Below are the histograms relating to the production of compounds obtained from the above simulation.



Chapter 3

Icao database integration

The method presented in the following pages is designed for the occurrences in which it is desired to carry out analysis of emissions by categories of engines that are not present in the ICAO databank. It is therefore necessary to be able to obtain emission indices in order to expand the existing database. It should be noted that the resulting indices refer to the pre-established flight conditions and therefore do not always coincide with the SL conditions. Furthermore, only and exclusively the cases in which the propulsion system operates in ON-DESIGN conditions are considered. Considering the multitude of existing engines, and the variety of them, the performance characteristics are analyzed for the gas generator group, which unites all types of propulsion systems.

3.1 Generic gas generator performance analysis

The proposed alternative method aims at calculating the emissions of pollutants for those engines not contained in the ICAO database and on which, not knowing the characteristics of the respective LTO cycles -in terms of pollutants-, it is not possible to apply the fuel flow method 2 previously proposed.

Specifically, by analyzing the performance on design of the engine, it is possible to obtain the values of T_2° and P_2° and then replace them in the appropriate relations for the calculation of NOx, CO, CO₂ and HC. In literature, these variables are indicated with T_3° and p_3° for a different denomination of the stages of the gas generator.

The starting point is the thermal balance in the combustion chamber, by equating the corresponding enthalpy difference between sections 2 and 3 (inlet and outlet of the combustor) and the thermal power:

$$w_f H_i \eta_b = (w_f + w_a) c_p' (T_3^\circ - T_2^\circ) \quad (3.1)$$

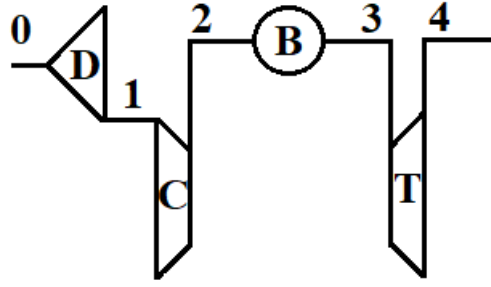


Figure 3.1 Generic gas generator scheme

Subsequently, the factor α can be introduced equal to the ratio between the air flow rate entering the combustor w_a and the fuel flow rate w_f , obtaining:

$$\frac{\eta_b H_i}{(1 + \alpha)c'_p} = T_3^\circ - T_2^\circ \quad (3.2)$$

Where T_2° is the total temperature in the combustion chamber inlet equivalent to the temperature leaving the compression stage and instead T_3° is the temperature leaving the combustor, and will be the degree of freedom of the system.

The specific heat c'_p of the fluid after combustion can be expressed as:

$$\left\{ \begin{array}{l} c'_p = \bar{c}_p + \frac{1+\alpha_{st}}{1+\alpha} (54.818 + 0.7535T_m^\circ) \\ \bar{c}_p = 946 + \frac{0.1844}{2} (T_3^\circ + T_2^\circ) \end{array} \right. \quad (3.3)$$

$$\bar{c}_p = 946 + \frac{0.1844}{2} (T_3^\circ + T_2^\circ) \quad (3.4)$$

Where \bar{c}_p is an average, approximate value. Substituting the relation 4 into the 3 we obtain:

$$c'_p = 946 + \frac{0.1844}{2} (T_3^\circ + T_2^\circ) + \frac{1 + \alpha_{st}}{1 + \alpha} [54.818 + 0.07535 \left(\frac{T_3^\circ + T_2^\circ}{2} \right)] \quad (3.5)$$

$$c'_p = T_3^\circ \left(\frac{0.1844}{2} + 0.037675 \frac{1 + \alpha_{st}}{1 + \alpha} \right) + T_2^\circ \left(\frac{0.1844}{2} + 0.037675 \frac{1 + \alpha_{st}}{1 + \alpha} \right) + 946 + 54.818 \frac{1 + \alpha_{st}}{1 + \alpha}$$

(3.6)

At this point, for the sake of simplicity, a coefficient k is introduced, the terms of which can be considered constant even when the environmental conditions vary

$$k = \frac{0.1844}{2} + 0.03765 \frac{1 + \alpha_{st}}{1 + \alpha} \quad (3.7)$$

Obtaining a simplified expression for the specific heat at the end of the combustion process

$$c'_p = kT_3^\circ + kT_2^\circ + 946 + 54.818 \frac{1 + \alpha_{st}}{1 + \alpha} \quad (3.8)$$

Relation 2 is now reported, resulting from the heat balance in the combustor

$$\frac{\eta_b H_i}{(1 + \alpha)} = T_3^\circ c'_p - T_2^\circ c'_p \quad (3.9)$$

And the expression 8 is replaced in the 9, developing the products

$$\frac{\eta_b H_i}{(1 + \alpha)} = T_3^\circ \left[kT_3^\circ + kT_2^\circ + 946 + 54.818 \frac{1 + \alpha_{st}}{1 + \alpha} \right] - T_2^\circ \left[kT_3^\circ + kT_2^\circ + 946 + 54.818 \frac{1 + \alpha_{st}}{1 + \alpha} \right] \quad (3.10)$$

$$\begin{aligned} \frac{\eta_b H_i}{(1 + \alpha)} = & -kT_3^\circ T_2^\circ - kT_2^{\circ 2} - 946T_2^\circ - 54.818 \frac{1 + \alpha_{st}}{1 + \alpha} T_2^\circ + kT_3^{\circ 2} + kT_3^\circ T_2^\circ + 946T_3^\circ \\ & + 54.818 \frac{1 + \alpha_{st}}{1 + \alpha} T_3^\circ = 0 \end{aligned} \quad (3.11)$$

$$\frac{\eta_b H_i}{(1 + \alpha)} = -kT_2^{\circ 2} - T_2^\circ (946 + 54.818 \frac{1 + \alpha_{st}}{1 + \alpha}) + kT_3^{\circ 2} + T_3^\circ (946 + 54.818 \frac{1 + \alpha_{st}}{1 + \alpha}) = 0 \quad (3.12)$$

For simplicity of discussion, also in this case a coefficient h is introduced, in order to obtain an equation in which only the terms related to T_2° and T_3° are evident

$$h = (946 + 54.818 \frac{1 + \alpha_{st}}{1 + \alpha}) \quad (3.13)$$

$$\frac{\eta_b H_i}{(1+\alpha)} = -kT_2^{\circ 2} - hT_2^{\circ} + kT_3^{\circ 2} + hT_3^{\circ} \quad (3.14)$$

$$kT_2^{\circ 2} + hT_2^{\circ} - kT_3^{\circ 2} - hT_3^{\circ} + \frac{\eta_b H_i}{(1+\alpha)} = 0 \quad (3.15)$$

The second degree equation in T_2° is solved by appropriately replacing the characteristic parameters of the fuel used:

- η_b overall combustion efficiency. In this case it is considered unitary since an ideal combustion is assumed in order to obtain the maximum value of carbon dioxide produced by the reaction;
- H_i lower heating value (LHV). It is a characteristic parameter of the type of fuel used;
- $\frac{1+\alpha_{st}}{1+\alpha}$ represents a relationship that links the stoichiometric dosage (i.e. the air to fuel ratio for which there are no residues of any kind in the combustion) and the real one, but since, as will be discussed later, the combustion efficiency will be considered unitary, this ratio can also be considered unitary;
- T_3° temperature of the flow leaving the combustion chamber. It corresponds to the throttle, the degree of freedom of the motor adjustment, a variable that must be chosen arbitrarily in order to carry out the analysis. There are temperature values that allow the optimization of the combustion process together with the optimization of the engine performance.

At this point, the isentropic that links the pressure jump and the temperature jump in the compression stage is introduced

$$\frac{T_2^{\circ}}{T_1^{\circ}} = \left(\frac{p_2^{\circ}}{p_1^{\circ}}\right)^{\frac{\gamma-1}{\gamma}} \quad (3.16)$$

By making the appropriate replacements

$$T_2^{\circ} = T_1^{\circ}(\beta_c)^{\frac{\gamma-1}{\gamma}} = T_0^{\circ}(\beta_c)^{\frac{\gamma-1}{\gamma}} = T_0\left(1 + \frac{\gamma-1}{2}M_0^2\right)(\beta_c)^{\frac{\gamma-1}{\gamma}} \quad (3.17)$$

In the last expression it was possible to replace T_1° with T_0° since the air intake of the engine is considered in most cases, as an adiabatic first approximation, therefore heat exchanges can be neglected. Subsequently, the total temperature can be replaced with the relationship that binds it to the static temperature, to the Mach corresponding to the actual flight speed and to the coefficient of adiabatic expansion $\gamma = \frac{c_p}{c_v}$.

As for the second unknown p_2° , it can be obtained as the product of significant pressure ratios, station by station:

$$p_2^\circ = \frac{p_2^\circ p_1^\circ p_0^\circ}{p_1^\circ p_0^\circ p_0^\circ} p_0 \quad (3.18)$$

That is in other words

$$p_2^\circ = \beta_c \varepsilon_d \frac{p_0^\circ}{p_0} p_0 \quad (3.19)$$

Again, by exploiting the isentropic relations, the ratio between total and static pressure in station 0 can be written, as

$$\frac{p_0^\circ}{p_0} = \left(1 + \frac{\gamma - 1}{2} M_0^2\right)^{\frac{\gamma}{\gamma - 1}} \quad (3.20)$$

And replacing in the eq. 19

$$p_2^\circ = \beta_c \varepsilon_d \left(1 + \frac{\gamma - 1}{2} M_0^2\right)^{\frac{\gamma}{\gamma - 1}} p_0 \quad (3.21)$$

The pressure loss of the air intake is assumed unitary $\varepsilon_d = 1$, thus assuming an ideal efficiency of the intake itself.

At this point we have found two expressions (eq. 3.21 and 3.17) that allow us to derive the two unknown terms, T_2° p_2° , which, when suitably substituted in the relations obtained by the methods presented later, will allow an estimate of the pollutant emissions in on-design conditions at pre-established altitude and flight conditions.

The only data required to carry out the analysis consist of:

- Dilution ratio of fuels in stoichiometric and non-stoichiometric conditions. Typically the value of $f = 1/\alpha$ is around 0.03³¹. Nonetheless as anticipated, ratio $\frac{1+\alpha_{st}}{1+\alpha}$ will be considered unitary assuming an ideal combustion;
- Characteristics of the fuel, specifically lower heating value (H_i);
- Ambient condition (T_0 , p_0) flight speed (M_0);
- Compression ratio (β_c);

³¹ D. A. Sullivan, P. A. Mas, *A Critical Review of NOx Correlations for Gas Turbine Combustors*, in American Society of Mechanical Engineers, pp 3, 1976

In order to reduce the number of unknown variables required by the model presented, equation 17 and equation 15 are used by making a substitution. Assuming a temperature T_3° at the end of combustion (corresponding with the engine adjustment lever) it is possible to obtain the compression ratio β_c .

$$k[T_0(1 + \frac{\gamma-1}{2}M_0^2)(\beta_c)^{\frac{\gamma-1}{\gamma}}]^2 + hT_0(1 + \frac{\gamma-1}{2}M_0^2)(\beta_c)^{\frac{\gamma-1}{\gamma}} - kT_3^{\circ 2} - hT_3^\circ + \frac{\eta_b H_i}{(1+\alpha)} = 0 \quad (3.22)$$

$$kT_0^2(1 + \frac{\gamma-1}{2}M_0^2)^2[(\beta_c)^{\frac{\gamma-1}{\gamma}}]^2 + hT_0(1 + \frac{\gamma-1}{2}M_0^2)(\beta_c)^{\frac{\gamma-1}{\gamma}} - kT_3^{\circ 2} - hT_3^\circ + \frac{\eta_b H_i}{(1+\alpha)} = 0 \quad (3.23)$$

From the previous one, solved as a second degree equation in $(\beta_c)^{\frac{\gamma-1}{\gamma}}$ it is possible to obtain the value of β_c , which appropriately replaced in eq. 3.17 and 3.21, will allow to calculate the two main variables unknowns, p_2° and T_2° . The steps suggested above ensure the dependence of the calculation on the fuel characteristics. In fact, the use of a different lower heating value will allow the analysis of emissions to be carried out as a result of the choice of traditional fuels or alternative fuels (biofuels).

In order to apply the method in its entirety, as is evident, knowledge of some parameters that are not easy to hypothesize or to know a priori is required. References have been searched in the literature which allow these variables to be approximated to experimentally obtained average values in relation to other performance characteristics. For example, in the graph below³² it is possible to establish a dependence between flight speed and the ratio between thrust and air mass.

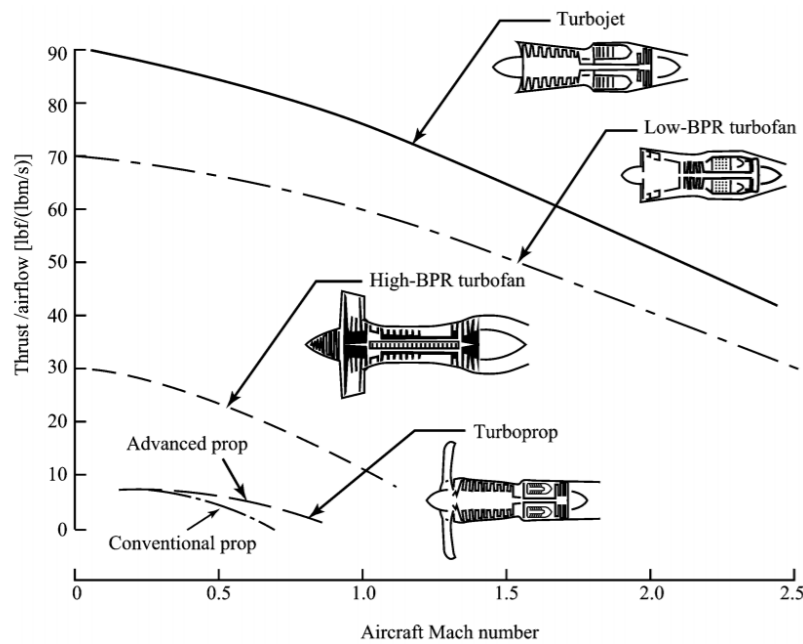


Figure 3.2 Thrust characteristics of typical aircraft engine

³² Jack D. Mattingly, *Elements of gas turbine propulsion*, 6 ed, New Delhi, Tata McGraw Hill, 2013, pp 28

In the hypothesis of obtaining the emission indexes for a standard LTO cycle, the flight speed and consequently the speed of the flow entering the exoreactor can be obtained by consulting this graph, after obtaining thrust and air flow values.

Instead, to obtain the mass of air, an approximation is made. According to Hill et al. , the dosage (ratio between fuel flow and air flow into the engine) is typically equal 0.05. Knowing at this point alpha and the fuel flow, which is also obtained from the ICAO prescriptions that describe the standard cycle, it is possible to obtain the air flow.

Once these values have been obtained, the graph presented above can be exploited to derive the maximum speed to be replaced in M0 for the calculation of emissions in each phase.

For the purposes of the calculation, knowledge of the fuel flow in the various phases of the LTO cycle is required. As in the previous chapter, this information is set as input parameters. Or alternatively knowledge of the SFC is required:

$$\dot{w}_f = SFC \cdot T \quad (3.24)$$

$$SFC = 25e^{(-0.05 BPR)} [mg/(N s)] \quad (3.25)$$

Remembering that in the 4 distinct phases the thrust is equivalent to a fraction of the nominal (100% take-off, 85% climb-out, 30% approach, 0.07% idle).

3.2 Emission calculation with correlation based models

The methods used for the emissions calculation all have a direct dependence on the two parameters just calculated, p_2° e T_2° , and have been drawn from previous and different studies. They are called correlation based models

3.2.1 Nitrogen Oxides

For the calculation of nitrogen oxide emissions NO_x ³³, the method proposed by AECMA³⁴ - European Association of Aerospace Industries- is used:

$$EINO_x = 2 + 28.5 \sqrt{\frac{p_2^\circ}{3100}} \exp\left(\frac{T_2^\circ - 825}{250}\right) \quad (3.26)$$

Alternatively, it is possible to calculate the emissions of nitrogen oxides using the method proposed by NASA³⁵.

$$EINO_x = 33.2 \left(\frac{p_2^\circ}{432.7}\right)^{0.4} \exp\left(\frac{T_2^\circ - 459.67 - 1027}{349.9} + \frac{6.29 - 6.3}{53.2}\right) \quad (3.27)$$

p_2° = Pressure of compressor exit (psia)

T_2° = Temperature of compressor exit (Deg R)

The NASA NEPP³⁶ code used an equation to predict the NOx emissions at any given power setting, based on the engine's T3 and P3 conditions. The NASA NEPP data is not intended to replicate any particular engine.

³³ N. Chandrasekaran, A. Gue, *Study of Prediction Methods for NOx Emission from Turbofan Engines*, in *Journal of Propulsion and Power*, v. 28, n. 1, pp 179, Feb. 2012

³⁴ Green, J. E., *Greener by Design: The Technology Challenge*, *Aeronautical Journal*, v. 106, n. 1056, pp. 57–113 Feb. 2002

³⁵ David L. Daggett, *Water Misting and Injection of Commercial Aircraft Engines to Reduce Airport Nox*, pp 4, Seattle, Washington, National Aeronautics and Space Administration, 2004

³⁶ The NEPP Program generates technical knowledge and recommendations about electrical, electronic, electromechanical (EEE) part performance, application, failure modes, test methods, reliability and supply chain quality within the context of NASA space flight missions and hardware. This information is made available to the NASA and high-reliability aerospace community through publications, web pages and links published on the website

3.2.2 Carbon dioxide and water

The carbon dioxide emissions CO_2 are calculated following the routine of the COPERT³⁷ method (presented previously). In summary, this method exploits the combustion and molecular characteristics, therefore it is independent from the performance of the propulsion system if not for the dependence on the fuel flow rate.

Furthermore, to obtain the estimate of the maximum production of carbon dioxide, a unitary combustion efficiency is assumed $\eta_b = 1$, as anticipated in the discussion.

$$E_{CO_2,t,k}^{CALC} = 44.011 \frac{FC_{t,k}^{CALC}}{12.011 + 1.008 r_{H:C,t} + 16 r_{O:C,t}} \quad (3.28)$$

Alternatively, since carbon dioxide and water are the main products of hydrocarbon combustion, their quantity emitted is directly proportional to the mass of fuel burned. In the hypothesis of using an A-1 jet fuel, characterized by the molecular formula $C_{12}H_{23}$, 3156g of CO_2 and 1237g of H_2O are produced for 1 kg of fuel. At this point it would be enough to have the amount of fuel used. However, this method is valid only and exclusively for the calculation of emissions deriving from the use of traditional fuels, thus not allowing a differentiated treatment for biofuels. For this reason it is preferable to first use the COPERT method (universal), and at the same time the calculation of water vapor will be subtracted from the analysis.

3.2.3 Carbon monoxide

CO is formed by incomplete combustion and/or dissociation of CO_2 . Concentrations are high at idle because of inadequate mixing, low temperature and fuel quenching on the walls³⁸. The CO carbon monoxide emissions are obtained from the relationship discussed by *Deidewig et al.*³⁹. Specifically, the emission index of carbon monoxide is related to the total volume of the combustor V_c and to the combustor loading parameter θ_c :

$$EICO = f(V_c, \theta_c) \quad (3.29)$$

con V_c combustor chamber volume, and

$$\theta_c = \frac{p_2^{\circ n} e^{\frac{T_2^{\circ}}{b}}}{w_{air}} \quad (3.30)$$

³⁷ A. Bernetti, R. De Lauretis, G. Iarocci, F. Lena, R. Marra Campanale, E. Taurino, *Inventario nazionale delle emissioni e disaggregazione provinciale*, Istituto Superiore per la Ricerca e Protezione Ambientale, 2010

³⁸ F. W. Lipfert, *Correlation of Gas Turbine Emissions Data*, in *American Society of Mechanical Engineers*, pp 3, 1972

³⁹ F. Deidewig, A. Doppelheuer, M. Lecht, *Methods to assess aircraft engine emissions in flight*, ICAS-96-4.1.2, pp 136, DLR, Institute for Propulsion Technology, Cologne, Germany, 1996

where $n \cong 1.75$ and $b \cong 300\text{ K}$

Ad esempio, per il caso particolare del CF6-50C2 (che verrà riportato in seguito), l'eq. 4.27 si traduce in:

$$EICO = 369.6 \left(\frac{1}{\theta_c}\right)^2 - 14.96 \frac{1}{\theta_c} + 0.647 \quad (3.31)$$

The German Aerospace Center (DLR) uses this alternative method. Emissions of CO and HC result from incomplete combustion and are mostly produced at low power settings of the engines, where the efficiency of the combustion process is low.⁴⁰

This equation is obtained by Lefebvre correlation, that contains many common variables that effect CO levels include combustor inlet pressure, pressure drop, primary zone temperature (T_{pz}) and a ratio between the volume of combustion (V_c) and the volume needed for fuel to evaporate (V_e)⁴¹.

$$EICO = \frac{86 \cdot \dot{m}_a \cdot T_{pz} \cdot \exp(-0.0035T_{pz})}{(V_c - V_e) \sqrt{\frac{\Delta p_2}{p_2}} p_3^{1.5}} \quad (3.32)$$

3.2.4 Hydrocarbons

The combustion residues, which occur when the combustion efficiency is not uniform, are mainly made up of CO and HC⁴². Specifically, unburnt HC hydrocarbons represent on average about 1% of total CO₂ and H₂O emissions. Their production is closely linked, as anticipated, to the efficiency of the combustion process η_c

$$\eta_c = 100 - 0.1 \cdot EIHC - 0.02334 \cdot EICO [\%] \quad (3.33)$$

This formulation, proposed by the German Aerospace Center (DLR) uses an alternative method, and is valid if the combustion efficiency is known a priori. In the case under

⁴⁰ Martin Shaefer, *Methodologies for Aviation Emission Calculation – A comparison of alternative approaches towards 4D global inventories*, Berlin University of Technology, 2006

⁴¹ Michael David Marchand, *Multi-Dimensional Carbon Monoxide Emissions Predictor for Preliminary Gas Turbine Combustor Design Optimization*, University of Toronto, 2013

⁴² C.J. Evers, D. Addleton, K. Atkinson, M.J. Broomhead, R. Christou, T. Elliff, R. Falk, I. Gee, D.S. Lee, C. Marizy, S. Michot, J. Middel, P. Newton, P. Norman, D. Raper, N. Stanciou, *AERO2K Global Aviation Emissions Inventories for 2002 and 2025*, Tech. Rep. QinetiQ, Farnborough, UK, 2004

consideration, however, there is no information regarding the process, in fact for the calculation of carbon dioxide emissions the efficiency is assumed to be unitary (which would exclude the generation of unburnt substances). Consequently, we are limited to calculating the hydrocarbon emissions as a fraction of the total amount of carbon dioxide and water emissions, and being an entity less than 0.01%, the calculation of the EIHC will be neglected.

3.3 Example of calculation

Below is an example of calculating the emissions on the LTO cycle of the CF6-50C2, a 230.5 kN nominal thrust engine. According to the ICAO requirements for the LTO cycle, the fuel flow for each phase is:

- T/O 2.36 kg/s
- C/O 1.94 kg/s
- App 0.668 kg/s
- Idle 0.163 kg/s

The main performance characteristics of the turbofan under consideration are summarized below.

CF6-50C2		
Manufacturer: GE : General Electric		
Application: A300B2-203, A300B4-103/-103F/-2C/-203/-203F, A300C4-203, A300F4-203, DC-10-30/-30F/-30F(CF), A300B1 (option), KC-10A		
Composition: 1 / 3B / 14 / 2 / - / 4		Nb of shafts = 2
$D_{fan} = 2.195 \text{ m} = 86.4 \text{ in}$	$D = 2.667 \text{ m}$	$L = \text{m}$
$W_{eng} = 3960 \text{ kg} = 8730 \text{ lb}$	$= 105 \text{ in}$	$= \text{in}$
Static Sea Level:		
$T_{ssl} = 230500 \text{ N}$	$T_{ssl}^{AB} = \text{N}$	Cruise:
$= 51818 \text{ lbf}$	$= \text{lbf}$	
$SFC_{ssl} = 1.05 \cdot 10^{-5} \text{ (kg/s)/N}$	$SFC_{ssl}^{AB} = \text{(kg/s)/N}$	
$= 0.37 \text{ (lb/h)/lbf}$	$= \text{(lb/h)/lbf}$	
$\dot{w}_{ssl} = 669.5 \text{ kg/s} = 1476 \text{ lb/s}$		
$BPR = 4.31$	$OPR = 30.4$	
$FPR =$	$TET = ^\circ\text{K}$	
		$T_{cr} = 51399 \text{ N}$
		$= 11555 \text{ lbf}$
		$SFC_{cr} = 1.79 \cdot 10^{-5} \text{ (kg/s)/N}$
		$= 0.63 \text{ (lb/h)/lbf}$
		$\dot{w}_{cr} = \text{kg/s} = \text{lb/s}$
		$OPR_{cr} =$
		$M_{cr} = 0.8, h_{cr} = 10668 \text{ m}$

Figure 3.3 Specifications for General Electric CF6-50C2⁴³

As evident in the analysis carried out previously, knowledge of the end-of-combustion temperature TET , T_3° is of fundamental importance. In this case the maximum value is equal to 1650° K . This temperature affects the dosage f , the ratio between fuel flow and air flow. In static conditions at sea level, the fuel flow rate will be equal to the product of SFC and thrust:

⁴³ Elodie Roux, *Turbofan and Turbojet Engines Database Handbook*, Edition Elodie Roux, Blagnac, France, 2007

$$\dot{w}_f = SFC \cdot T = 230500 \cdot 1.05 \cdot 10^{-5} = 2.42 \text{ kg/s} \quad (3.34)$$

This value is obtained using the maximum thrust value, for the purpose of analyzing the LTO cycle, and corresponds to the takeoff conditions; it will therefore be necessary to jointly evaluate the fuel flow rate in relation to the reduced thrust values for climb out, approach and taxi.

$$\dot{w}_{f,CO} = SFC \cdot T \cdot 0.85 = 195925 \cdot 1.05 \cdot 10^{-5} = 2.057 \text{ kg/s} \quad (3.35)$$

$$\dot{w}_{f,App} = SFC \cdot T \cdot 0.3 = 69150 \cdot 1.05 \cdot 10^{-5} = 0.7260 \text{ kg/s} \quad (3.36)$$

$$\dot{w}_{f,Idle} = SFC \cdot T \cdot 0.07 = 16135 \cdot 1.05 \cdot 10^{-5} = 0.1694 \text{ kg/s} \quad (3.37)$$

The values just calculated differ slightly from those provided within the ICAO database.

Another parameter to be obtained in order to complete the performance analysis and consequently the emissions is the speed of the flow entering the engine, M_0 . For this purpose the graph presented previously is exploited (Figure 3.2). From the data obtained in the literature, the end-of-combustion temperature in the specific engine considered varies between a minimum of 1450 ° K and 1663 ° K⁴⁴. By making an approximation and assuming that the trend between the thrust generated and the TIT is linear and linked by direct proportionality, the value of T_3 can be obtained for each phase of the LTO cycle. Consequently, through the graph of the following figure (3.4), it is possible to obtain the dosage ratio corresponding to each turbine inlet temperature, assuming that the temperature of the reagents is 400 ° K.

⁴⁴ C56–50A Engines, *Aircraft Engineering and Aerospace Technology*, Vol. 43 No. 9, pp. 28-32, 1971

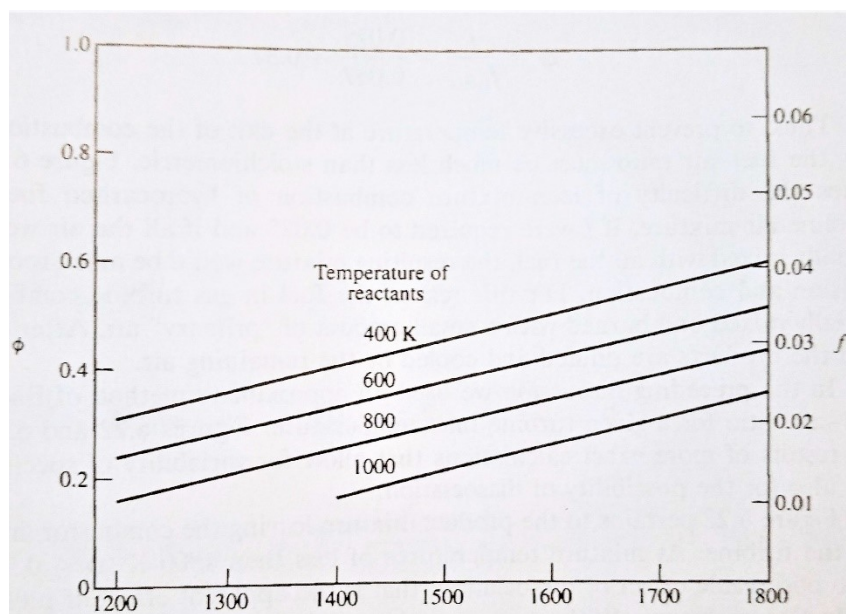


Figure 3.4 Trend of the dosage f as a function of the end-of-combustion temperature⁴⁵

At this point, all the data necessary to carry out the analysis are available. The table shows the input data (marked by blue) and the simulation results (in red).

Table 3.1 Data and results of simulation for CF6-50C2 using Jet-A1

	Take Off	Climb Out	Approach	Idle
Thrust [N]	230500	195925	69150	16135
T3 [K]	1663	1631.5	1513.9	1464.9
f	0.037	0.036	0.0335	0.033
Fuel Flow [kg/s]	2.42	2.057	0.726	0.1694
M0	0.05	0.23	0.5	0.3
T2 [K]	462.658	458.175	399.323	355.7437
p2 [bar]	4.616	4.464	2.757	1.84
Beta c	4.494	3.799	2.617	1.855
EICO [g/kg]	0.75	0.45	22.959	20.778
EICO2 [kg]	8.557	7.034	2.422	0.591
EINOx [g/kg]	24.284	23.407	14.265	9.7
EIHC [g/kg]	0.536	0.553	0.457	0.705

The trends in CO and HC emissions are in contrast with those of CO₂ and NO_x: while the former decrease as T_2 , T_3 and fuel flow increase, the latter are characterized by proportional growth.

⁴⁵ P. G. Hill, C. R. Peterson, *Mechanics and thermodynamics of propulsion*, pp 244, Addison-Wesley Publishing Company, Cambridge, 1992

The data thus obtained, as anticipated at the beginning of the chapter, refer to an LTO cycle for the certification and control of pollutants, and will be the starting point for the application of the Fuel Flow Method 2 of chapter 2.

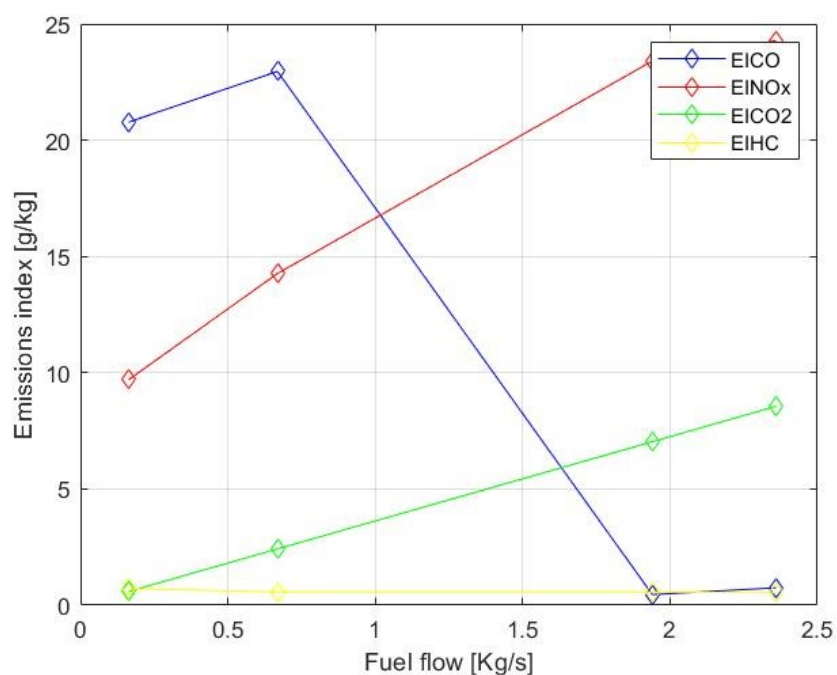


Figure 3.5 Emissions index related to F.F. for CO, CO₂, HC and Nox for JET-A1

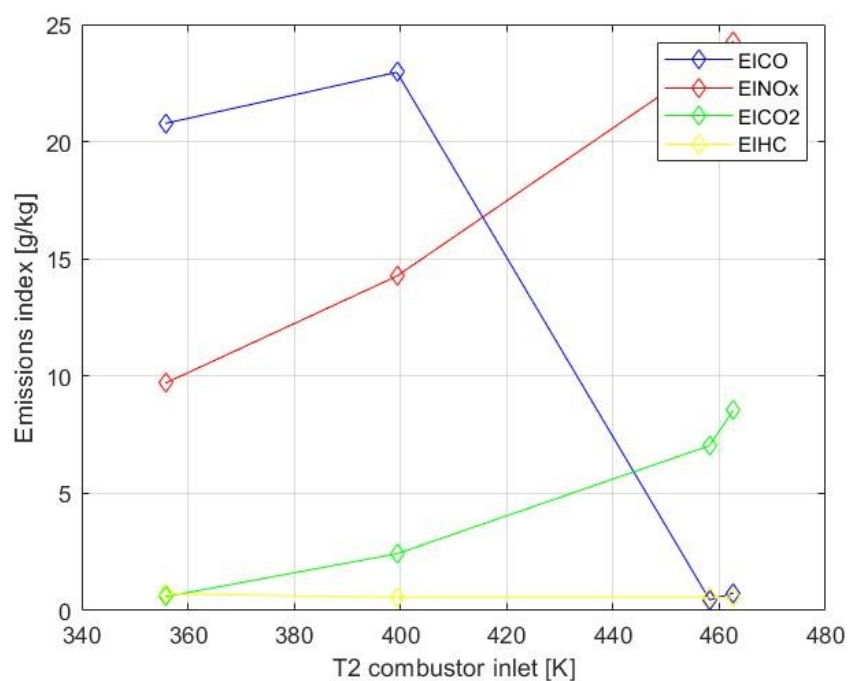


Figure 3.6 Emissions index related to T2 for CO, CO₂, HC and Nox for JET-A1

The advantage, in addition to the possibility of inserting exoreactors in the database for which there are no experimental data, lies in the fact of being able to carry out analyzes also for performances deriving from the use of unconventional fuels, thanks to the dependence of the calculation of temperatures and pressures in the combustor by the characteristics of the fuel itself, and specifically its efficiency and its lower calorific value.

Below is the analysis of the performance of the same engine, in the event that it is powered by a mixture made up of 100% CSPK

As known, LHV becomes an utmost factor that influence engine thrust. Besides LHV, heat capacity of the combustible mixture (fuel and air) (C_p) could be another factor that might affect the amount of thrust generated by an aircraft engine. By the way, the LHV of JSPK is higher than that of CSPK (JSPK = 44.3 MJ/kg and CSPK = 44.0 MJ/kg)⁴⁶.

Again, the data used and the results obtained are presented in the table below.

Table 3.2 Data and results of simulation for CF6-50C2 using CSPK

	Take Off	Climb Out	Approach	Idle
Thrust [N]	230500	195925	69150	16135
T3 [K]	1663	1631.5	1513.9	1464.9
f	0.037	0.036	0.0335	0.033
Fuel Flow [kg/s]	2.36	1.94	0.668	0.163
M0	0.23	0.5	0.3	0.05
T2 [K]	443.713	439.705	381.857	338.351
p2 [bar]	3.987	3.863	2.357	1.544
Beta c	4.494	3.799	2.617	1.855
EICO [g/kg]	16.374	13.865	77.31	72.67
EICO2 [kg]	8.557	7.034	2.422	0.591
EINOx [g/kg]	20.775	20.094	12.248	8.2665
EIHC [g/kg]	0.4498	0.4803	0.4763	0.6178

⁴⁶ Effects of biofuels properties on aircraft engine performance, in *Aircraft Engineering and aerospace technology*, 87(5), pp 437-443, Emerald, 2013

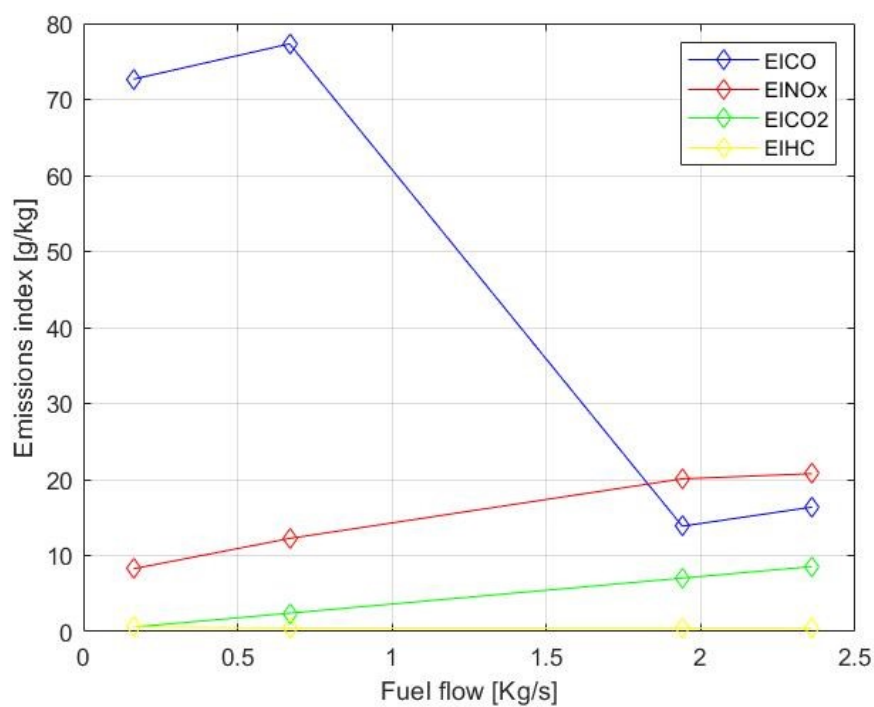


Figure 3.7 Emissions index related to F.F. for CO, CO₂, HC and Nox for CSPK

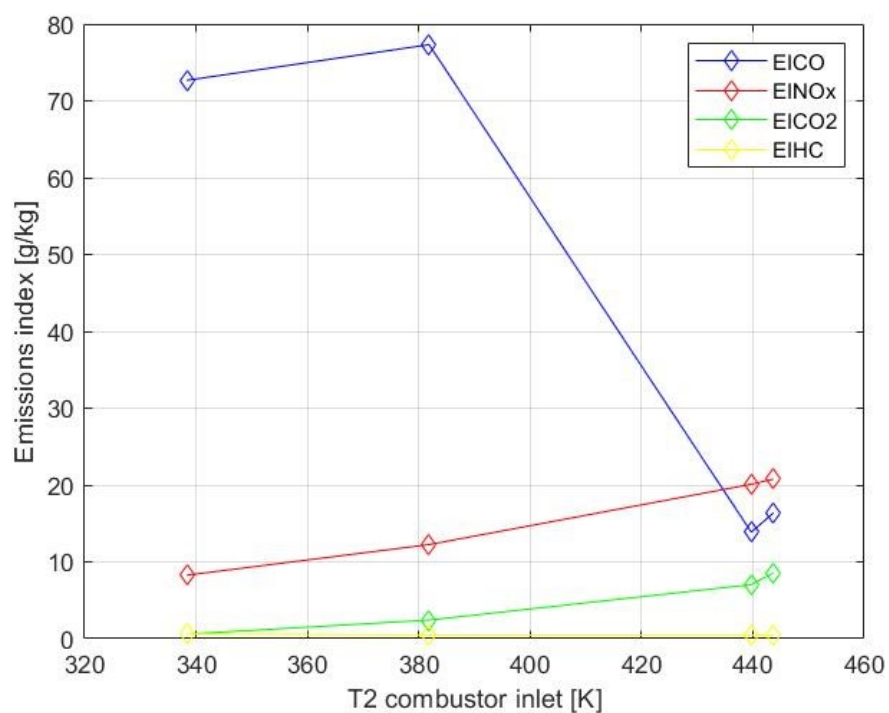


Figure 3.8 Emissions index related to T2 for CO, CO₂, HC and Nox for CSPK

Conclusions

From the results obtained, it is possible to deduce that the application of biofuels, as anticipated by previous studies, is not so advantageous from the point of view of the reductions in emissions produced during an operating cycle as a consequence of the combustion process.

The different lower heating value, which varies from fuel to fuel, and the different molecular structure affect the process inside the combustion chamber, causing the variation of fundamental parameters of pressure, temperature and dosage ratio between the amount of air and fuel burned.

In fact, some of the pollutants, such as nitrogen oxides, are emitted in larger quantities if we compare the use of biofuels to the use of A1 jet fuel. The other compounds, and specifically the carbon monoxides, on the other hand, have an opposite trend, decreasing both in the case of CSPK and JSPK. The latter are calculated only if the combustion process is not considered ideal. Otherwise, an estimation of carbon dioxide emissions can be made, which according to the estimates made is reduced, albeit to a negligible extent, due to the effect of the application of alternative fuels. For this last occurrence, it should be specified that the advantage in the use of biofuels does not lie so much in the analysis of the operating cycle and combustion, but if we refer to the well to wheel life cycle, they certainly offer a valid application in order to reduce the environmental impact of air transport. In fact, being fuels obtained from biomass, they guarantee a limitation of carbon emissions deriving from the characteristic extraction and production processes of kerosene. They are therefore considered potential substitutes for the power supply of aeronautical engines, both for the environmental advantages and for their potential application regardless of the changes to be made to the configuration of pre-existing aircraft.

Appendix A

Matlab code for Fuel Flow method application

```

%% LETTURA DATI DA DATABASE
clear all
clc
disp('LETTURA DATI DA DATABASE');
spinta_tot=input('inserisci valore di spinta compreso tra 40 e 500
kN:');
numero_motori=input('inserisci numero motori (2 o 4):');
carburantel=input('Inserire 1 per JET-A, 2 per CSPK, 3 per JSPK:');
spinta=spinta_tot/numero_motori;
% CASO JET-A
if carburantel==1
    [JETA,
MOTORE]=xlsread('DATABASE\DATABASE_JETA.xlsx','A2:AF620');
    i=0;
    for i=1:619
        if spinta==JETA(i,1) || (spinta>JETA(i,1) &&
spinta<JETA(i+1,1))
            mot=MOTORE(i, 1:2)
            EIHC_TO=JETA(i,2);
            EIHC_CO=JETA(i,3);
            EIHC_App=JETA(i,4);
            EIHC_Idle=JETA(i,5);
            EICO2_TO=JETA(i,7);
            EICO2_CO=JETA(i,8);
            EICO2_App=JETA(i,9);
            EICO2_Idle=JETA(i,10);
            EICO_TO=JETA(i,11);
            EICO_CO=JETA(i,12);
            EICO_App=JETA(i,13);
            EICO_Idle=JETA(i,14);
            EINOx_TO=JETA(i,16);
            EINOx_CO=JETA(i,17);
            EINOx_App=JETA(i,18);
            EINOx_Idle=JETA(i,19);
            WF_SL_TO=JETA(i,21);
            WF_SL_CO=JETA(i,22);
            WF_SL_App=JETA(i,23);
            WF_SL_Idle=JETA(i,24);
        else
            i=i+1;
        end
    end
end

%CASO CSPK
elseif carburantel==2
    blend=input('Inserire percentuale miscela (20, 40, 60, 80,
100):');

    if blend==20
        [CSPK20,
MOTORE]=xlsread('DATABASE\DATABASE_CSPK20.xlsx','A2:AR620');
        i=0;
        for i=1:619

```

```

        if spinta==CSPK20(i,1) ||
(spinta>CSPK20(i,1) && spinta<CSPK20(i+1,1))
            mot=MOTORE(i, 1:2)
            EIHC_TO=CSPK20(i,2);
            EIHC_CO=CSPK20(i,3);
            EIHC_App=CSPK20(i,4);
            EIHC_Idle=CSPK20(i,5);
            EICO2_TO=CSPK20(i,7);
            EICO2_CO=CSPK20(i,8);
            EICO2_App=CSPK20(i,9);
            EICO2_Idle=CSPK20(i,10);
            EICO_TO=CSPK20(i,11);
            EICO_CO=CSPK20(i,13);
            EICO_App=CSPK20(i,15);
            EICO_Idle=CSPK20(i,17);
            EINOx_TO=CSPK20(i,20);
            EINOx_CO=CSPK20(i,22);
            EINOx_App=CSPK20(i,24);
            EINOx_Idle=CSPK20(i,26);
            WF_SL_TO=CSPK20(i,29);
            WF_SL_CO=CSPK20(i,31);
            WF_SL_App=CSPK20(i,33);
            WF_SL_Idle=CSPK20(i,35);
        else
            i=i+1;
        end
    end

elseif blend==40
    [CSPK40,
MOTORE]=xlsread('DATABASE\DATABASE_CSPK40.xlsx','A2:AR620');
    i=0;
    for i=1:619
        if spinta==CSPK40(i,1) ||
(spinta>CSPK40(i,1) && spinta<CSPK40(i+1,1))
            mot=MOTORE(i, 1:2)
            EIHC_TO=CSPK40(i,2);
            EIHC_CO=CSPK40(i,3);
            EIHC_App=CSPK40(i,4);
            EIHC_Idle=CSPK40(i,5);
            EICO2_TO=CSPK40(i,7);
            EICO2_CO=CSPK40(i,8);
            EICO2_App=CSPK40(i,9);
            EICO2_Idle=CSPK40(i,10);
            EICO_TO=CSPK40(i,11);
            EICO_CO=CSPK40(i,13);
            EICO_App=CSPK40(i,15);
            EICO_Idle=CSPK40(i,17);
            EINOx_TO=CSPK40(i,20);
            EINOx_CO=CSPK40(i,22);
            EINOx_App=CSPK40(i,24);
            EINOx_Idle=CSPK40(i,26);
            WF_SL_TO=CSPK40(i,29);
            WF_SL_CO=CSPK40(i,31);
            WF_SL_App=CSPK40(i,33);
            WF_SL_Idle=CSPK40(i,35);
        else

```

```

        i=i+1;
    end
end

elseif blend==60
    [CSPK60,
MOTORE]=xlsread('DATABASE\DATABASE_CSPK60.xlsx','A2:AR620');
    i=0;
    for i=1:619
        if spinta==CSPK60(i,1) ||
(spinta>CSPK60(i,1) && spinta<CSPK60(i+1,1))
            mot=MOTORE(i, 1:2)
            EIHC_TO=CSPK60(i,2);
            EIHC_CO=CSPK60(i,3);
            EIHC_App=CSPK60(i,4);
            EIHC_Idle=CSPK60(i,5);
            EICO2_TO=CSPK60(i,7);
            EICO2_CO=CSPK60(i,8);
            EICO2_App=CSPK60(i,9);
            EICO2_Idle=CSPK60(i,10);
            EICO_TO=CSPK60(i,11);
            EICO_CO=CSPK60(i,13);
            EICO_App=CSPK60(i,15);
            EICO_Idle=CSPK60(i,17);
            EINOx_TO=CSPK60(i,20);
            EINOx_CO=CSPK60(i,22);
            EINOx_App=CSPK60(i,24);
            EINOx_Idle=CSPK60(i,26);
            WF_SL_TO=CSPK60(i,29);
            WF_SL_CO=CSPK60(i,31);
            WF_SL_App=CSPK60(i,33);
            WF_SL_Idle=CSPK60(i,35);
        else
            i=i+1;
        end
    end

elseif blend==80
    [CSPK80,
MOTORE]=xlsread('DATABASE\DATABASE_CSPK80.xlsx','A2:AR620');
    i=0;
    for i=1:619
        if spinta==CSPK80(i,1) ||
(spinta>CSPK80(i,1) && spinta<CSPK80(i+1,1))
            mot=MOTORE(i, 1:2)
            EIHC_TO=CSPK80(i,2);
            EIHC_CO=CSPK80(i,3);
            EIHC_App=CSPK80(i,4);
            EIHC_Idle=CSPK80(i,5);
            EICO2_TO=CSPK80(i,7);
            EICO2_CO=CSPK80(i,8);
            EICO2_App=CSPK80(i,9);
            EICO2_Idle=CSPK80(i,10);
            EICO_TO=CSPK80(i,11);
            EICO_CO=CSPK80(i,13);
            EICO_App=CSPK80(i,15);
            EICO_Idle=CSPK80(i,17);

```

```

        EINOx_TO=CSPK80(i,20);
        EINOx_CO=CSPK80(i,22);
        EINOx_App=CSPK80(i,24);
        EINOx_Idle=CSPK80(i,26);
        WF_SL_TO=CSPK80(i,29);
        WF_SL_CO=CSPK80(i,31);
        WF_SL_App=CSPK80(i,33);
        WF_SL_Idle=CSPK80(i,35);
    else
        i=i+1;
    end
end

elseif blend==100
    [CSPK100,
MOTORE]=xlsread('DATABASE\DATABASE_CSPK100.xlsx','A2:AR620');
    i=0;
    for i=1:619
        if spinta==CSPK100(i,1) ||
(spinta>CSPK100(i,1) && spinta<CSPK100(i+1,1))
            mot=MOTORE(i, 1:2)
            EIHC_TO=CSPK100(i,2);
            EIHC_CO=CSPK100(i,3);
            EIHC_App=CSPK100(i,4);
            EIHC_Idle=CSPK100(i,5);
            EICO2_TO=CSPK100(i,7);
            EICO2_CO=CSPK100(i,8);
            EICO2_App=CSPK100(i,9);
            EICO2_Idle=CSPK100(i,10);
            EICO_TO=CSPK100(i,11);
            EICO_CO=CSPK100(i,13);
            EICO_App=CSPK100(i,15);
            EICO_Idle=CSPK100(i,17);
            EINOx_TO=CSPK100(i,20);
            EINOx_CO=CSPK100(i,22);
            EINOx_App=CSPK100(i,24);
            EINOx_Idle=CSPK100(i,26);
            WF_SL_TO=CSPK100(i,29);
            WF_SL_CO=CSPK100(i,31);
            WF_SL_App=CSPK100(i,33);
            WF_SL_Idle=CSPK100(i,35);
        else
            i=i+1;
        end
    end
end

end

%CASO JSPK
elseif carburantel==3
    blend=input('Inserire percentuale miscela (20, 40, 60, 80,
100):');
    if blend==20
        [JSPK20,
MOTORE]=xlsread('DATABASE\DATABASE_JSPK20.xlsx','A2:AR620');
        i=0;

```

```

        for i=1:619
            if spinta==JSPK20(i,1) || (spinta>JSPK20(i,1) &&
spinta<JSPK20(i+1,1))
                mot=MOTORE(i, 1:2)
                EIHC_TO=JSPK20(i,2);
                EIHC_CO=JSPK20(i,3);
                EIHC_App=JSPK20(i,4);
                EIHC_Idle=JSPK20(i,5);
                EICO2_TO=JSPK20(i,7);
                EICO2_CO=JSPK20(i,8);
                EICO2_App=JSPK20(i,9);
                EICO2_Idle=JSPK20(i,10);
                EICO_TO=JSPK20(i,11);
                EICO_CO=JSPK20(i,13);
                EICO_App=JSPK20(i,15);
                EICO_Idle=JSPK20(i,17);
                EINOx_TO=JSPK20(i,20);
                EINOx_CO=JSPK20(i,22);
                EINOx_App=JSPK20(i,24);
                EINOx_Idle=JSPK20(i,26);
                WF_SL_TO=JSPK20(i,29);
                WF_SL_CO=JSPK20(i,31);
                WF_SL_App=JSPK20(i,33);
                WF_SL_Idle=JSPK20(i,35);
            else
                i=i+1;
            end
        end

    elseif blend==40
        [JSPK40,
MOTORE]=xlsread('DATABASE\DATABASE_JSPK40.xlsx','A2:AR620');
        i=0;
        for i=1:619
            if spinta==JSPK40(i,1) ||
(spinta>JSPK40(i,1) && spinta<JSPK40(i+1,1))
                mot=MOTORE(i, 1:2)
                EIHC_TO=JSPK40(i,2);
                EIHC_CO=JSPK40(i,3);
                EIHC_App=JSPK40(i,4);
                EIHC_Idle=JSPK40(i,5);
                EICO2_TO=JSPK40(i,7);
                EICO2_CO=JSPK40(i,8);
                EICO2_App=JSPK40(i,9);
                EICO2_Idle=JSPK40(i,10);
                EICO_TO=JSPK40(i,11);
                EICO_CO=JSPK40(i,13);
                EICO_App=JSPK40(i,15);
                EICO_Idle=JSPK40(i,17);
                EINOx_TO=JSPK40(i,20);
                EINOx_CO=JSPK40(i,22);
                EINOx_App=JSPK40(i,24);
                EINOx_Idle=JSPK40(i,26);
                WF_SL_TO=JSPK40(i,29);
                WF_SL_CO=JSPK40(i,31);
                WF_SL_App=JSPK40(i,33);
                WF_SL_Idle=JSPK40(i,35);
            end
        end
    end
end

```

```

        else
            i=i+1;
        end
    end

    elseif blend==60
        [JSPK60,
MOTORE]=xlsread('DATABASE\DATABASE_JSPK60.xlsx','A2:AR620');
        i=0;
        for i=1:619
            if spinta==JSPK60(i,1) ||
(spinta>JSPK60(i,1) && spinta<JSPK60(i+1,1))
                mot=MOTORE(i, 1:2)
                EIHC_TO=JSPK60(i,2);
                EIHC_CO=JSPK60(i,3);
                EIHC_App=JSPK60(i,4);
                EIHC_Idle=JSPK60(i,5);
                EICO2_TO=JSPK60(i,7);
                EICO2_CO=JSPK60(i,8);
                EICO2_App=JSPK60(i,9);
                EICO2_Idle=JSPK60(i,10);
                EICO_TO=JSPK60(i,11);
                EICO_CO=JSPK60(i,13);
                EICO_App=JSPK60(i,15);
                EICO_Idle=JSPK60(i,17);
                EINOx_TO=JSPK60(i,20);
                EINOx_CO=JSPK60(i,22);
                EINOx_App=JSPK60(i,24);
                EINOx_Idle=JSPK60(i,26);
                WF_SL_TO=JSPK60(i,29);
                WF_SL_CO=JSPK60(i,31);
                WF_SL_App=JSPK60(i,33);
                WF_SL_Idle=JSPK60(i,35);
            else
                i=i+1;
            end
        end

    elseif blend==80
        [JSPK80,
MOTORE]=xlsread('DATABASE\DATABASE_JSPK80.xlsx','A2:AR620');
        i=0;
        for i=1:619
            if spinta==JSPK80(i,1) ||
(spinta>JSPK80(i,1) && spinta<JSPK80(i+1,1))
                mot=MOTORE(i, 1:2)
                EIHC_TO=JSPK80(i,2);
                EIHC_CO=JSPK80(i,3);
                EIHC_App=JSPK80(i,4);
                EIHC_Idle=JSPK80(i,5);
                EICO2_TO=JSPK80(i,7);
                EICO2_CO=JSPK80(i,8);
                EICO2_App=JSPK80(i,9);
                EICO2_Idle=JSPK80(i,10);
                EICO_TO=JSPK80(i,11);
                EICO_CO=JSPK80(i,13);
                EICO_App=JSPK80(i,15);
            end
        end
    end
end

```

```

        EICO_Idle=JSPK80(i,17);
        EINOx_TO=JSPK80(i,20);
        EINOx_CO=JSPK80(i,22);
        EINOx_App=JSPK80(i,24);
        EINOx_Idle=JSPK80(i,26);
        WF_SL_TO=JSPK80(i,29);
        WF_SL_CO=JSPK80(i,31);
        WF_SL_App=JSPK80(i,33);
        WF_SL_Idle=JSPK80(i,35);
    else
        i=i+1;
    end
end

elseif blend==100

[JSPK100,MOTORE]=xlsread('DATABASE\DATABASE_JSPK100.xlsx','A2:AR620'
);
    i=0;
    for i=1:619
        if spinta==JSPK100(i,1) ||
(spinta>JSPK100(i,1) && spinta<JSPK100(i+1,1))
            mot=MOTORE(i, 1:2)
            EIHC_TO=JSPK100(i,2);
            EIHC_CO=JSPK100(i,3);
            EIHC_App=JSPK100(i,4);
            EIHC_Idle=JSPK100(i,5);
            EICO2_TO=JSPK100(i,7);
            EICO2_CO=JSPK100(i,8);
            EICO2_App=JSPK100(i,9);
            EICO2_Idle=JSPK100(i,10);
            EICO_TO=JSPK100(i,11);
            EICO_CO=JSPK100(i,13);
            EICO_App=JSPK100(i,15);
            EICO_Idle=JSPK100(i,17);
            EINOx_TO=JSPK100(i,20);
            EINOx_CO=JSPK100(i,22);
            EINOx_App=JSPK100(i,24);
            EINOx_Idle=JSPK100(i,26);
            WF_SL_TO=JSPK100(i,29);
            WF_SL_CO=JSPK100(i,31);
            WF_SL_App=JSPK100(i,33);
            WF_SL_Idle=JSPK100(i,35);
        else
            i=i+1;
        end
    end
end

end

end

WF_SL=[WF_SL_TO WF_SL_CO WF_SL_App WF_SL_Idle];
EICO2_SL=[EICO2_TO EICO2_CO EICO2_App EICO2_Idle];
EICO_SL=[EICO_TO EICO_CO EICO_App EICO_Idle];
EIHC_SL=[EIHC_TO EIHC_CO EIHC_App EIHC_Idle];
EINOx_SL=[EINOx_TO EINOx_CO EINOx_App EINOx_Idle];

```

```
figure
loglog(WF_SL, EICO_SL, '- r *', WF_SL, EICO2_SL, '- y *', WF_SL,
EIHC_SL, '- b *', WF_SL, EINOx_SL, '- g *')
grid on;
xlabel("Portata combustibile S.L");
ylabel("Emissioni [g/kg]");
title("Andamento emissioni");
legend("CO_s_l", "CO2_s_l", "HC_s_l", "NOx_s_l");
```

%% CALCOLO EMISSIONI LTO CYCLE

```
%emissioni_tot_hc_idle= WF_SL_Idle*EIHC_Idle*1560;
%emissioni_tot_hc_to= WF_SL_TO*EIHC_TO*42;
%emissioni_tot_hc_co= WF_SL_CO*EIHC_CO*132;
%emissioni_tot_hc_app= WF_SL_App*EIHC_App*240;
```

```
%emissioni_tot_co_idle= WF_SL_Idle*EICO_Idle*1560;
%emissioni_tot_co_to= WF_SL_TO*EICO_TO*42;
%emissioni_tot_co_co= WF_SL_CO*EICO_CO*132;
%emissioni_tot_co_app= WF_SL_App*EICO_App*240;
```

```
%emissioni_tot_co2_idle= WF_SL_Idle*EICO2_Idle*1560;
%emissioni_tot_co2_to= WF_SL_TO*EICO2_TO*42;
%emissioni_tot_co2_co= WF_SL_CO*EICO2_CO*132;
%emissioni_tot_co2_app= WF_SL_App*EICO2_App*240;
```

```
%emissioni_tot_nox_idle= WF_SL_Idle*EINOx_Idle*1560;
%emissioni_tot_nox_to= WF_SL_TO*EINOx_TO*42;
%emissioni_tot_nox_co= WF_SL_CO*EINOx_CO*132;
%emissioni_tot_nox_app= WF_SL_App*EINOx_App*240;
```

```
WF_SL=[0 numero_motori*WF_SL_TO numero_motori*WF_SL_CO
numero_motori*WF_SL_App numero_motori*WF_SL_Idle];
EICO2_SL=[0 numero_motori*EICO2_TO numero_motori*EICO2_CO
numero_motori*EICO2_App numero_motori*EICO2_Idle];
EICO_SL=[0 numero_motori*EICO_TO numero_motori*EICO_CO
numero_motori*EICO_App numero_motori*EICO_Idle];
EIHC_SL=[0 numero_motori*EIHC_TO numero_motori*EIHC_CO
numero_motori*EIHC_App numero_motori*EIHC_Idle];
EINOx_SL=[0 numero_motori*EINOx_TO numero_motori*EINOx_CO
numero_motori*EINOx_App numero_motori*EINOx_Idle];
```

```
vett_t=[0 1560 1560 1602 1602 1734 1734 1974];
vett_em_CO=[EICO_SL(2) EICO_SL(2) EICO_SL(3) EICO_SL(3) EICO_SL(4)
EICO_SL(4) EICO_SL(5) EICO_SL(5)];
vett_em_HC=[EIHC_SL(2) EIHC_SL(2) EIHC_SL(3) EIHC_SL(3) EIHC_SL(4)
EIHC_SL(4) EICO_SL(5) EICO_SL(5)];
vett_em_NOx=[EINOx_SL(2) EINOx_SL(2) EINOx_SL(3) EINOx_SL(3)
EINOx_SL(4) EINOx_SL(4) EINOx_SL(5) EINOx_SL(5)];
vett_em_CO2=[EICO2_SL(2) EICO2_SL(2) EICO2_SL(3) EICO2_SL(3)
EICO2_SL(4) EICO2_SL(4) EICO2_SL(5) EICO2_SL(5)];
```

```
figure
plot(vett_t,vett_em_CO, '- r *', 'LineWidth',3);
title("EI CO LTO CYCLE");
xlabel("Time [s]");
```

```

ylabel("EI [g/kg]");
grid on

figure
plot(vett_t,vett_em_HC, '- r *','LineWidth',3);
title("EI HC LTO CYCLE");
xlabel("Time [s]");
ylabel("EI [g/kg]");
grid on

figure
plot(vett_t,vett_em_CO2, '- r *','LineWidth',3);
title("EI CO2 LTO CYCLE");
xlabel("Time [s]");
ylabel("EI [g/kg]");
grid on

figure
plot(vett_t,vett_em_NOx, '- r *','LineWidth',3);
title("EI NOx LTO CYCLE");
xlabel("Time [s]");
ylabel("EI [g/kg]");
grid on

%% CALCOLO EMISSIONI AL VARIARE DELLA QUOTA / FUEL FLOW METHOD
disp('CALCOLO EMISSIONI AL VARIARE DELLA QUOTA / FUEL FLOW METHOD');
disp('INSERIMENTO CARATTERISTICHE MISSION PROFILE');

M_idle = input('Inserire MACH massimo di taxi :');
M_TO = input('inserire MACH massimo di takeoff :');
M_CO = input('inserire MACH massimo di climbout :');
M_cruise = input('inserire MACH massimo di cruise :');
M_app = input('inserire MACH massimo di approach :');
M_landing = input('Inserire MACH massimo atterraggio :');

t_idle=input('Inserire durata manovra di taxi [s]:');
t_TO=input('Inserire durata manovra di decollo [s]:');
t_CO=input('Inserire durata totale climb out [s]:');
t_cruise=input('inserire durata totale crociera [s]:');
t_app=input('Inserire durata totale manovra avvicinamento [s]:');
t_landing=input('Inserire durata totale atterraggio [s]:');

z0_idle= input('inserire quota di decollo: ');
zf_idle= z0_idle;
z0_TO= z0_idle;
zf_TO= input('inserire quota fine manovra decollo: ');
z0_CO= zf_TO;
zf_CO= input('inserire quota fine climb out: ');
z0_cruise=zf_CO;
zf_cruise=z0_cruise;
z0_app= zf_CO;
zf_app= input('inserire quota di fine approach: ');
z0_landing=zf_app;
zf_landing=z0_landing;

```

```

Consumo_idle=input('Inserire portata combustibile della manovra di
taxi:');
Consumo_TO=input('Inserire portata combustibile della manovra di
decollo:');
Consumo_CO=input('Inserire portata combustibile della manovra di
climb-out:');
Consumo_cruise=input('Inserire portata combustibile in crociera:');
Consumo_app=input('Inserire portata combustibile della manovra di
avvicinamento:');
Consumo_landing=input('Inserire portata combustibile di
atterraggio:');

% PLOT DEL MISSION PROFILE
t_vett=[0 t_idle t_idle+t_TO t_idle+t_TO+t_CO
t_idle+t_TO+t_CO+t_cruise t_idle+t_TO+t_CO+t_cruise+t_app
t_idle+t_TO+t_CO+t_cruise+t_app+t_landing];
z_vett=[0 0 zf_TO zf_CO zf_CO zf_app 0];
figure
plot(t_vett,z_vett);

dt=1;
t_tot=t_idle+t_TO+t_CO+t_cruise+t_app+t_landing;
for t=1:t_tot

    if t<t_idle

        n=t_idle;
        M=linspace(0,M_idle,n);
        z=linspace(1,zf_idle,n);
        T_amb=(15-0.0065.*z)+273.15;
        p_amb=1.01325.*(T_amb./288.15).^5.25;
        theta_amb=T_amb./518.67;
        delta_amb=p_amb./14.696;
        Consumo_idle_vet=linspace(0, Consumo_idle,n);

Wf_sl_idle=Consumo_idle_vet.*(theta_amb.^4.5)./(delta_amb).*exp(0.2.
*(M.^2));
        F1=interp1(WF_SL, EICO2_SL, Wf_sl_idle, 'linear', 'extrap');
        G1=interp1(WF_SL, EICO_SL, Wf_sl_idle, 'linear', 'extrap');
        H1=interp1(WF_SL, EIHC_SL, Wf_sl_idle, 'linear', 'extrap');
        I1=interp1(WF_SL, EINOx_SL, Wf_sl_idle, 'linear', 'extrap');
        CO2_TOT_IDLE = F1.*((theta_amb.^3.3)./(delta_amb.^1.02));
        CO_TOT_IDLE =
G1.*((theta_amb.^3.3)./(delta_amb.^1.02)).*Consumo_idle;%*(Consumo_i
dle*t_idle);%calcolo g di emissioni tramite fuel flow. Se non
effettuassi correzione, avrei g/kg come nel database
        HC_TOT_IDLE =
H1.*((theta_amb.^3.3)./(delta_amb.^1.02)).*Consumo_idle;%*(Consumo_i
dle*t_idle);
        NOx_TOT_IDLE =
I1.*(((delta_amb.^1.02)./(theta_amb.^3.3)).^0.5).*Consumo_idle;%*(Co
nsumo_idle*t_idle);

    elseif (t>t_idle && t<(t_idle+t_TO))

        n=t_TO;

```

```

M=linspace(M_idle, M_TO ,n);
z=linspace(zf_idle,zf_TO,n);
T_amb=(15-0.0065.*z)+273.15;
p_amb=1.01325.*(T_amb./288.15).^5.25;
theta_amb=T_amb./518.67;
delta_amb=p_amb./14.696;
Consumo_TO_vet=linspace(Consumo_idle, Consumo_TO,n);

Wf_sl_TO=Consumo_TO_vet.*(theta_amb.^4.5)./(delta_amb).*exp(0.2.*(M.
^2));

F2=interp1(WF_SL, EICO2_SL, Wf_sl_TO, 'linear', 'extrap');
G2=interp1(WF_SL, EICO_SL, Wf_sl_TO, 'linear', 'extrap');
H2=interp1(WF_SL, EIHC_SL, Wf_sl_TO, 'linear', 'extrap');
I2=interp1(WF_SL, EINOx_SL, Wf_sl_TO, 'linear', 'extrap');
CO2_TOT_TO = F2.*((theta_amb.^3.3)./(delta_amb.^1.02));
CO_TOT_TO =
G2.*((theta_amb.^3.3)./(delta_amb.^1.02)).*Consumo_TO;%*(Consumo_TO*
t_TO);
HC_TOT_TO =
H2.*((theta_amb.^3.3)./(delta_amb.^1.02)).*Consumo_TO;%*(Consumo_TO*
t_TO);
NOx_TOT_TO =
I2.*(((delta_amb.^1.02)./(theta_amb.^3.3)).^0.5).*Consumo_TO;%*(Cons
umo_TO*t_TO);

elseif (t>(t_idle+t_TO) && t<(t_idle+t_TO+t_CO))
n=t_CO;
M=linspace(M_TO, M_CO ,n);
z=linspace(zf_TO,zf_CO,n);

T_amb=(15-0.0065.*z)+273.15;
p_amb=1.01325.*(T_amb./288.15).^5.25;
theta_amb=T_amb./518.67;
delta_amb=p_amb./14.696;
Consumo_CO_vet=linspace(Consumo_TO, Consumo_CO, n);

Wf_sl_CO=Consumo_CO_vet.*(theta_amb.^4.5)./(delta_amb).*exp(0.2.*(M.
^2));

F3=interp1(WF_SL, EICO2_SL, Wf_sl_CO, 'linear', 'extrap');
G3=interp1(WF_SL, EICO_SL, Wf_sl_CO, 'linear', 'extrap');
H3=interp1(WF_SL, EIHC_SL, Wf_sl_CO, 'linear', 'extrap');
I3=interp1(WF_SL, EINOx_SL, Wf_sl_CO, 'linear', 'extrap');
CO2_TOT_CO = F3.*((theta_amb.^3.3)./(delta_amb.^1.02));
CO_TOT_CO =
G3.*((theta_amb.^3.3)./(delta_amb.^1.02)).*Consumo_CO;%*(Consumo_CO*
t_CO);
HC_TOT_CO =
H3.*((theta_amb.^3.3)./(delta_amb.^1.02)).*Consumo_CO;%*(Consumo_CO*
t_CO);
NOx_TOT_CO =
I3.*(((delta_amb.^1.02)./(theta_amb.^3.3)).^0.5).*Consumo_CO;%*(Cons
umo_CO*t_CO);

```

```

elseif (t>(t_idle+t_TO+t_CO) && t<(t_idle+t_TO+t_CO+t_cruise))

    n=t_cruise;
    M=(M_cruise*ones(n,1))';%linspace(M_CO,M_cruise,n);
    z=(zf_cruise*ones(n,1))'; %linspace(zf_cruise,zf_cruise,n);
    T_amb=(15-0.0065.*z)+273.15;
    p_amb=1.01325.*(T_amb./288.15).^5.25;
    theta_amb=T_amb./518.67;
    delta_amb=p_amb./14.696;
    Consumo_cruise_vet=
(Consumo_cruise*ones(n,1))';%linspace(Consumo_CO,Consumo_cruise, n);

Wf_sl_cruise=Consumo_cruise_vet.*(theta_amb.^4.5)./(delta_amb).*exp(
0.2.*(M.^2));
    F4=interp1(WF_SL, EICO2_SL, Wf_sl_cruise, 'linear',
'extrap');
    G4=interp1(WF_SL, EICO_SL, Wf_sl_cruise, 'linear',
'extrap');
    H4=interp1(WF_SL, EIHC_SL, Wf_sl_cruise, 'linear',
'extrap');
    I4=interp1(WF_SL, EINOx_SL, Wf_sl_cruise, 'linear',
'extrap');
    CO2_TOT_CRUISE = F4.*((theta_amb.^3.3)./(delta_amb.^1.02));
    CO_TOT_CRUISE =
G4.*((theta_amb.^3.3)./(delta_amb.^1.02)).*Consumo_cruise;%*(Consumo
_app*t_app);
    HC_TOT_CRUISE =
H4.*((theta_amb.^3.3)./(delta_amb.^1.02)).*Consumo_cruise;%*(Consumo
_app*t_app);
    NOx_TOT_CRUISE =
I4.*(((delta_amb.^1.02)./(theta_amb.^3.3)).^0.5).*Consumo_cruise;%*(
Consumo_app*t_app);

elseif (t>(t_idle+t_TO+t_CO+t_cruise) &&
t<(t_idle+t_TO+t_CO+t_cruise+t_app))

    n=t_app;
    M=linspace(M_cruise,M_app,n);
    z=linspace(zf_CO,zf_app,n);
    T_amb=(15-0.0065.*z)+273.15;
    p_amb=1.01325.*(T_amb./288.15).^5.25;
    theta_amb=T_amb./518.67;
    delta_amb=p_amb./14.696;
    Consumo_app_vet=linspace(Consumo_cruise,Consumo_app, n);

Wf_sl_app=Consumo_app_vet.*(theta_amb.^4.5)./(delta_amb).*exp(0.2.*(
M.^2));
    F5=interp1(WF_SL, EICO2_SL, Wf_sl_app, 'linear', 'extrap');
    G5=interp1(WF_SL, EICO_SL, Wf_sl_app, 'linear', 'extrap');
    H5=interp1(WF_SL, EIHC_SL, Wf_sl_app, 'linear', 'extrap');
    I5=interp1(WF_SL, EINOx_SL, Wf_sl_app, 'linear', 'extrap');
    CO2_TOT_APP = F5.*((theta_amb.^3.3)./(delta_amb.^1.02));
    CO_TOT_APP =
G5.*((theta_amb.^3.3)./(delta_amb.^1.02)).*Consumo_app;%*(Consumo_ap
p*t_app);

```

```

        HC_TOT_APP =
H5.*((theta_amb.^3.3)./(delta_amb.^1.02)).*Consumo_app;%*(Consumo_ap
p*t_app);
        NOx_TOT_APP =
I5.*(((delta_amb.^1.02)./(theta_amb.^3.3)).^0.5).*Consumo_app;%*(Con
sumo_app*t_app);

        elseif (t>(t_idle+t_TO+t_CO+t_cruise+t_app) &&
t<(t_idle+t_TO+t_CO+t_cruise+t_app+t_landing))

            n=t_landing;
            M=linspace(M_landing,0,n);
            z=linspace(zf_CO,zf_app,n);
            T_amb=(15-0.0065.*z)+273.15;
            p_amb=1.01325.*(T_amb./288.15).^5.25;
            theta_amb=T_amb./518.67;
            delta_amb=p_amb./14.696;
            Consumo_landing_vet=linspace(Consumo_landing,0,n);

Wf_sl_landing=Consumo_landing_vet.*(theta_amb.^4.5)./(delta_amb).*ex
p(0.2.*(M.^2));
            F6=interp1(WF_SL, EICO2_SL, Wf_sl_landing, 'linear',
'extrap');
            G6=interp1(WF_SL, EICO_SL, Wf_sl_landing, 'linear',
'extrap');
            H6=interp1(WF_SL, EIHCL_SL, Wf_sl_landing, 'linear',
'extrap');
            I6=interp1(WF_SL, EINOX_SL, Wf_sl_landing, 'linear',
'extrap');
            CO2_TOT_LANDING = F6.*((theta_amb.^3.3)./(delta_amb.^1.02));
            CO_TOT_LANDING =
G6.*((theta_amb.^3.3)./(delta_amb.^1.02)).*Consumo_landing;%*(Consum
o_app*t_app);
            HC_TOT_LANDING =
H6.*((theta_amb.^3.3)./(delta_amb.^1.02)).*Consumo_landing;%*(Consum
o_app*t_app);
            NOx_TOT_LANDING =
I6.*(((delta_amb.^1.02)./(theta_amb.^3.3)).^0.5).*Consumo_landing;%*
(Consumo_app*t_app);
            end

            t=t+dt;
        end

%% PLOT CONSUMI SU MISSION PROFILE
figure
grid on
CO2_TOT=[CO2_TOT_IDLE CO2_TOT_TO CO2_TOT_CO CO2_TOT_CRUISE
CO2_TOT_APP CO2_TOT_LANDING];
m=length(CO2_TOT);
T=linspace(0,t_tot,m);
yyaxis left

```

```

plot(T, CO2_TOT, 'r');
title("ANDAMENTO EMISSIONI CO2 NEL TEMPO DI MISSIONE");
xlabel("Tempo [s]");
ylabel("Emissioni [kg]");
hold on
yyaxis right
plot(t_vett,z_vett, 'b', 'LineWidth',2);
ylabel("Quota [10^3 m]");

figure
grid on
CO_TOT=[CO_TOT_IDLE CO_TOT_TO CO_TOT_CO CO_TOT_CRUISE CO_TOT_APP
CO_TOT_LANDING];
yyaxis left
plot(T, CO_TOT, 'r');
title("ANDAMENTO EMISSIONI CO NEL TEMPO DI MISSIONE");
xlabel("Tempo [s]");
ylabel("Emissioni [g/kg]");
hold on
yyaxis right
plot(t_vett,z_vett, 'b', 'LineWidth',2);
ylabel("Quota [10^3 m]");

figure
grid on
HC_TOT=[HC_TOT_IDLE HC_TOT_TO HC_TOT_CO HC_TOT_CRUISE HC_TOT_APP
HC_TOT_LANDING];
yyaxis left
plot(T, HC_TOT, 'r');
title("ANDAMENTO EMISSIONI HC NEL TEMPO DI MISSIONE");
xlabel("Tempo [s]");
ylabel("Emissioni [g/kg]");
hold on
yyaxis right
plot(t_vett,z_vett, 'b', 'LineWidth',2);
ylabel("Quota [10^3 m]");

figure
grid on
NOx_TOT=[NOx_TOT_IDLE NOx_TOT_TO NOx_TOT_CO NOx_TOT_CRUISE
NOx_TOT_APP NOx_TOT_LANDING];
yyaxis left
plot(T, NOx_TOT, 'r');
title("ANDAMENTO EMISSIONI TO NEL TEMPO DI MISSIONE");
xlabel("Tempo [s]");
ylabel("Emissioni [g/kg]");
hold on
yyaxis right
plot(t_vett,z_vett, 'b', 'LineWidth',2);
ylabel("Quota [10^3 m]");

%% PLOT ISTOGRAMMI CONSUMI
figure
K= [1 2 3 4 5 6];
CO= [ sum(CO_TOT_IDLE) sum(CO_TOT_TO) sum(CO_TOT_CO)
sum(CO_TOT_CRUISE) sum(CO_TOT_APP) sum(CO_TOT_LANDING) ];

```

```

bar(K, CO );
grid on;
xlabel("          IDLE          TAKE OFF          CLIMB          APPROACH");
ylabel("Emissioni [g]");
title("EMISSIONI TOTALI CO");
CO=sum(CO)

```

```

figure
HC= [ sum(HC_TOT_IDLE) sum(HC_TOT_TO) sum(HC_TOT_CO)
      sum(HC_TOT_CRUISE) sum(HC_TOT_APP) sum(HC_TOT_LANDING) ];
bar(K, HC );
grid on;
xlabel("          IDLE          TAKE OFF          CLIMB          APPROACH");
ylabel("Emissioni [g]");
title("EMISSIONI TOTALI HC");
HC=sum(HC)

```

```

figure
CO2= [ sum(CO2_TOT_IDLE) sum(CO2_TOT_TO) sum(CO2_TOT_CO)
       sum(CO2_TOT_CRUISE) sum(CO2_TOT_APP) sum(CO2_TOT_LANDING) ];
bar(K, CO2 );
grid on;
xlabel("          IDLE          TAKE OFF          CLIMB          APPROACH");
ylabel("Emissioni [kg]");
title("EMISSIONI TOTALI CO2");
CO2=sum(CO2)

```

```

figure
NOx= [ sum(NOx_TOT_IDLE) sum(NOx_TOT_TO) sum(NOx_TOT_CO)
       sum(NOx_TOT_CRUISE) sum(NOx_TOT_APP) sum(NOx_TOT_LANDING) ];
bar(K, NOx );
grid on;
xlabel("          IDLE          TAKE OFF          CLIMB          APPROACH");
ylabel("Emissioni [g]");
title("EMISSIONI TOTALI NOx");
NOx=sum(NOx)

```

Bibliography

- European aviation environmental report, Colonia, 2019, EASA
- L. Zhang., T. L. Butler, B. Yang, *Recent Trends, Opportunities and Challenges of Sustainable Aviation Fuel*, Green Energy to Sustainability: Strategies for Global Industries, ed. 1, 2020 John Wiley & Sons Ltd., 2020
- M. Shaefer, *Methodologies for aviation emissions calculation – A comparison of alternative approaches towards 4D global inventories*, Berlin University of Technology, German Aerospace Center (DLR), 2006
- D. Daggett, *Enabling Alternate Fuels for Commercial Aircraft*, Cranfield University, 2009
- *Intergovernmental Panel on Climate Change: Aviation and Global Atmosphere*, Cambridge university press, 1999
- A. Macintosh, L. Wallace, *International Aviation Emissions to 2025: can emissions be stabilised without restricting demand?*, Canberra, 2008, pp 5-6
- Strategic research and innovation agenda, 2017 update, Advisory Council for Aviation Research and Innovation in Europe, Derby, 2017, pp 48-60
- Environmental Protection, Annex 16, Vol. II, International Civil Aviation Organization, 3 ed., 2008
- J. D. Kinder, T. Rahmes, *Evaluation of bio-derived synthetic paraffinic kerosene (Bio-SPK)*, The boeing Company, Sustainable Biofuels Research & Technology Program, 2009
- A. P. Payan, M. Kirby, C. Y. Justin, D. N. Mavris, *Meeting Emissions Reduction Targets: A Probabilistic Lifecycle Assessment of the Production of Alternative Jet Fuels*, in American Institute of Aeronautics and Astronautics, School of Aerospace Engineering, Georgia Institute of Technology, Atlanta, 2015
- *Beginners guide to aviation biofuel*, Air Transport Action Group, 2009
- *The IATA technology roadmap report*, IATA, 3rd Edition, Montreal, QC, Canada, 2013
- *Sustainable aviation fuels guide*, ICAO, 2017
- *Useful information about conventional and alternate fuels and their feedstocks*, National Renewable Energy Lab, National Bioengineering Center, june 2004

- Lieberz, S., Germany Oilseeds and Products, Biodiesel in Germany – An Overview, USDA Report #GM2021, October 24, 2002
- D. Daggett, O. Hadaller, R. Hendricks, R. Walther, Alternative Fuels and their Potential Impact on Aviation, NASA, October 2006
- Bozel JJ. *The use of renewable feedstocks for the production of chemicals and materials-a brief overview of concepts*, National Renewable Energy Laboratory 2007
- Hari, Yaakob, Binitha, *Aviation biofuel from renewable resources: routes, opportunities and challenges*, renewable and sustainable energy reviews, 2015
- M. Nowak, R. Jasinski, M. Galant, *Implementation of the LTO cycle in flight conditions using FNPT II MCC simulator*, in IOP Conference series: materials science and engineering, pp 1-3
- *Annex 16: Environmental protection*, vol II: Aircraft Engine Emissions, 4th ed., ICAO
- *Effects of biofuels properties on aircraft engine performance*, in *Aircraft Engineering and aerospace technology*, 87(5), pp 437-443, Emerald, 2013
- Muhammad Hanafi Azami, M. Savill, *Comparative study of alternative biofuels on aircraft engine performance*, in *Journal of Aerospace Engineering*, vol. 231, 2017, pp 1509-1521
- B. Gawron, T. Bialecki, A. Janicka, T. Suchocki, *Combustion and Emissions Characteristics of the turbine engine fueled with HEFA Blends from different feedstock*, in *Energies*, vol. 1277, 2020, pp 1-12
- A. Bernetti, R. De Lauretis, G. Iarocci, F. Lena, R. Marra Campanale, E. Taurino, *Inventario nazionale delle emissioni e disaggregazione provinciale*, Istituto Superiore per la Ricerca e Protezione Ambientale, 2010
- D. Dubois, G. C. Paynter, Fuel Flow Method 2 for estimating Aircraft emissions, The Boeing Company, SAE international, 2006
- D. A. Sullivan, P. A. Mas, *A Critical Review of NOx Correlations for Gas Turbine Combustors*, in American Society of Mechanical Engineers, pp 3, 1976
- Jack D. Mattingly, *Elements of gas turbine propulsion*, 6 ed, New Delhi, Tata McGraw Hill, 2013, pp 28
- N. Chandrasekaran, A. Gaa, *Study of Prediction Methods for NOx Emission from Turbofan Engines*, in *Journal of Propulsion and Power*, v. 28, n. 1, pp 179, Feb. 2012
- Michael David Marchand, *Multi-Dimensional Carbon Monoxide Emissions Predictor for Preliminary Gas Turbine Combustor Design Optimization*, University of Toronto, 2013

- David L. Daggett, *Water Misting and Injection of Commercial Aircraft Engines to Reduce Airport Nox*, pp 4, Seattle, Washington, National Aeronautics and Space Administration, 2004
- A. Bernetti, R. De Lauretis, G. Iarocci, F. Lena, R. Marra Campanale, E. Taurino, *Inventario nazionale delle emissioni e disaggregazione provinciale*, Istituto Superiore per la Ricerca e Protezione Ambientale, 2010
- F. W. Lipfert, *Correlation of Gas Turbine Emissions Data*, in *American Society of Mechanical Engineers*, pp 3, 1972
- F. Deidewig, A. Doppelheuer, M. Lecht, *Methods to assess aircraft engine emissions in flight*, ICAS-96-4.1.2, pp 136, DLR, Institute for Propulsion Technology, Cologne, Germany, 1996
- Martin Shaefer, *Methodologies for Aviation Emission Calculation – A comparison of alternative approaches towards 4D global inventories*, Berlin University of Technology, 2006
- Michael David Marchand, *Multi-Dimensional Carbon Monoxide Emissions Predictor for Preliminary Gas Turbine Combustor Design Optimization*, University of Toronto, 2013
- C.J. Evers, D. Addleton, K. Atkinson, M.J. Broomhead, R. Christou, T. Elliff, R. Falk, I. Gee, D.S. Lee, C. Marizy, S. Michot, J. Middel, P. Newton, P. Norman, D. Raper, N. Stanciou, *AERO2K Global Aviation Emissions Inventories for 2002 and 2025*, Tech. Rep. QinetiQ, Farnborough, UK, 2004
- Elodie Roux, *Turbofan and Turbojet Engines Database Handbook*, Edition Elodie Roux, Blagnac, France, 2007
- C56–50A Engines, *Aircraft Engineering and Aerospace Technology*, Vol. 43 No. 9, pp. 28-32, 1971
- P. G. Hill, C. R. Peterson, *Mechanics and thermodynamics of propulsion*, pp 244, Addison-Wesley Publishing Company, Cambridge, 1992
- Effects of biofuels properties on aircraft engine performance, in *Aircraft Engineering and aerospace technology*, 87(5), pp 437-443, Emerald, 2013